

Variational decomposition autoencoding improves disentanglement of latent representations

Ioannis N. Ziogas¹, Aamna Al Shehhi¹, Ahsan H. Khandoker¹, Leontios J. Hadjileontiadis^{2,1}

¹Dept. of Biomedical Engineering, Khalifa University of Science and Technology, Abu Dhabi, UAE

²School of Electrical and Computer Engineering, Aristotle University of Thessaloniki, Thessaloniki, Greece

Abstract

Understanding the structure of complex, nonstationary, high-dimensional time-evolving signals is a central challenge in scientific data analysis. In many domains, such as speech and biomedical signal processing, the ability to learn disentangled and interpretable representations is critical for uncovering latent generative mechanisms. Traditional approaches to unsupervised representation learning, including variational autoencoders (VAEs), often struggle to capture the temporal and spectral diversity inherent in such data. Here we introduce variational decomposition autoencoding (VDA), a framework that extends VAEs by incorporating a strong structural bias toward signal decomposition. VDA is instantiated through variational decomposition autoencoders (DecVAEs), i.e., encoder-only neural networks that combine a signal decomposition model, a contrastive self-supervised task, and variational prior approximation to learn multiple latent subspaces aligned with time-frequency characteristics. We demonstrate the effectiveness of DecVAEs on simulated data and three publicly available scientific datasets, spanning speech recognition, dysarthria severity evaluation, and emotional speech classification. Our results demonstrate that DecVAEs surpass state-of-the-art VAE-based methods in terms of disentanglement quality, generalization across tasks, and the interpretability of latent encodings. These findings suggest that decomposition-aware architectures can serve as robust tools for extracting structured representations from dynamic signals, with potential applications in clinical diagnostics, human-computer interaction, and adaptive neurotechnologies.

Observing and disentangling the surrounding environment into basic properties -such as the shape of an object or the timbre of a sound- is a fundamental cognitive trait deeply embedded in intelligence hardwired into human brains since infancy [1]. Disentangled representations are crucial for the interpretability, generalization, and control in neural networks, as they enable robust encoding of underlying generative factors while suppressing noise and domain-irrelevant variation. For instance, healthy and dysarthric speech recognition [2, 3], emotional speech recognition [4], time series prediction [5, 6], separation of venous effects from neural activity [7], separation of cellular properties at the single-cell level [8], are all problems where high-dimensional, nonstationary inputs often conflate multiple latent factors. To uncover the underlying generative factors of these processes without prior knowledge about the task, unsupervised machine learning models typically assume statistical independence among latent variables [9]; this is a foundational bias in the unsupervised model of variational autoencoders (VAEs) [10]. VAEs encode independent generative factors into distinct dimensions of a latent space [11], but this assumption often fails in complex time-evolving processes, where generative factors are numerous, interdependent, and not well-defined (Fig. 1a).

Many methods have explored structural biases as a mechanism to promote disentanglement in such settings and achieve separation or decomposition of physically meaningful time-localized representations that have distinct spectral signatures [12]. This idea of decomposition is not new in signal processing, stirring an increasing exploration of inductive biases as structural interventions in unsupervised and self-supervised learning (SSL). For instance, time-contrastive learning (TCL) [13] hypothesizes nonlinear mixtures and time-evolving distributions, as a bias to disentangle time series events. Neural basis expansion analysis for interpretable time series (N-BEATS) [14] introduces inductive bias layers with task-specific weights to disentangle time series by performing a hierarchical decomposition of the input layer by layer. Contrastive learning of seasonal-trend (CoST) representations [6] views disentanglement as a gradual decomposition of the generative factors into seasonality and trend components utilizing layers with in-build Fourier transforms. Hence, imposing structural biases on the architecture or the learning objective is a mechanism that promotes disentanglement [15]. Nevertheless, while effective for task-specific performance, these methods are not explicitly designed to maximize disentanglement.

In the context of variational inference, disentanglement emerges indirectly from the pressure to approximate an orthogonal latent space governed by a multivariate Gaussian prior [11]. Extensions such as factorized hierarchical VAE (FHVAE) [16] and multiple filtered latent VAE (MFL-VAE) [17] introduce hierarchical time-scale modeling, while β -VAE [18], total correlation VAE (TCVAE) [19], and FactorVAE [20] explicitly regularize latent independence. However, these approaches lack structural priors on the generative process itself, limiting their applicability to complex nonstationary time-evolving processes with multiple factors. Here, we introduce variational decomposition autoencoding (VDA), a representation learning framework that advances disentanglement by embedding decomposition directly into the generative process (Fig. 1b). Its neural implementation, i.e., the variational decomposition autoencoder (DecVAE), is designed to uncover interpretable factors of variation in complex, time-evolving signals through a structured decomposition of latent subspaces (Fig. 1c,d, Supplementary Table 1). Unlike conventional VAEs, which assume independence among latent dimensions, VDA reformulates the generative model to incorporate frequency-resonant subspaces that precede and construct the target prior distribution (Fig. 1b). This architecture enables DecVAE to tie disentanglement explicitly to time-localized spectral dynamics, leveraging a signal decomposition model and deep encoder to approximate latent structure. To further enforce disentanglement, DecVAE integrates a self-supervised contrastive loss that guides latent components toward orthogonality and reconstructive fidelity, while maintaining Gaussian priors within each subspace (Fig. 1c). This mechanism promotes a principled separation of generative factors, allowing DecVAE to generalize across domains and recover physiologically grounded representations of complex time-evolving processes into physiological structure properties (e.g., vocal tract) or frequency alterations of these.

We evaluated DecVAEs on synthetic benchmarks and three real-world datasets spanning speech recognition, dysarthria severity progression, and emotion classification. Across all tasks, DecVAEs consistently outperformed state-of-the-art disentanglement models, demonstrating superior theoretical and empirical separation of latent factors, strong zero-shot generalization, and high interpretability of learned representations (see Results). These findings position VDA as a robust and versatile framework for disentangling the structure of complex generative processes. To enable researchers to leverage and further develop VDA, we have made all R/Python code publicly available in an easy-to-use format.

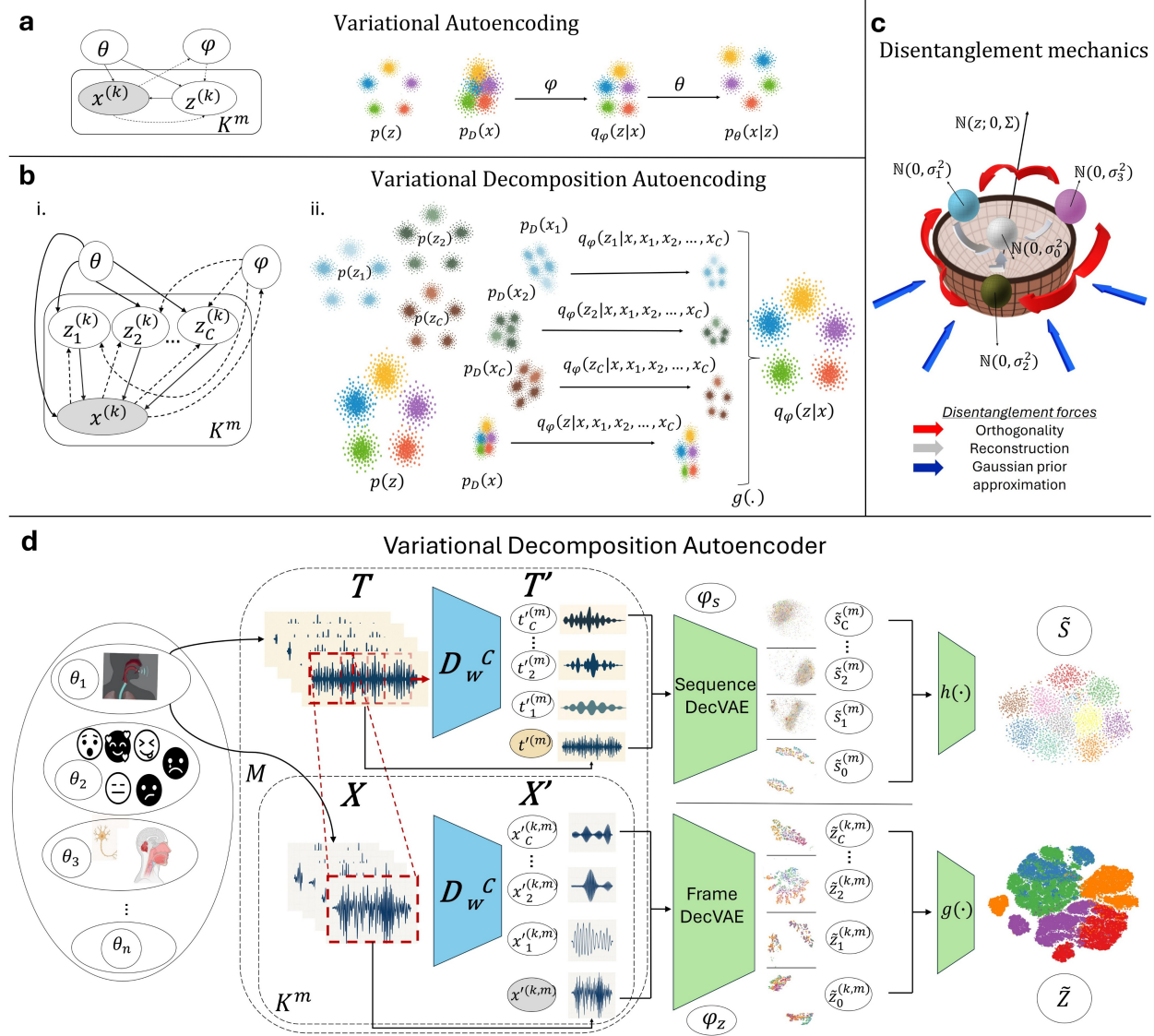


Fig. 1 | Variational decomposition autoencoding (VDA) uses a neural network encoder to approximate latent distributions assuming a decomposition generative process and novel disentanglement mechanics. **a**, variational autoencoding directed factor graph and illustration of processes for prior approximation (ϕ) and generation (θ). **b**, (i) directed factor graph for the proposed VDA; (ii) VDA assumes that the prior distribution $p(z)$ is a composition of multiple frequency-related priors $p(z_1), p(z_2), \dots, p(z_C)$ and aims to recover these multiple priors with a single recognition model q_ϕ . q_ϕ learns conditionally each subspace z_c based on information from other subspaces $\{z_1, z_2, \dots, z_{C-1}\}$ and the observed input distributions $p_D(x)$ and its decomposed components $\{p_D(x_1), p_D(x_2), \dots, p_D(x_C)\}$, and approximates the true prior $p(z)$ with $q_\phi(z|x)$ based on aggregation of subspaces z_c . **c**, VDA requires additional structural biases to the Gaussian prior approximation, found in the decomposition reconstruction and orthogonality dynamics that promote a unique structure of the latent space that disentangles. DecVAE trains by optimizing the decomposition evidence lower bound, an extension of the classic evidence lower bound with a self-supervised loss that embodies the structural bias of decomposition (detailed in Methods). **d**, The variational decomposition autoencoder (DecVAE) can generalize disentanglement across several domains θ_n (speech, emotion, dysarthria severity). DecVAE can optionally recover generative processes in more than one time scales K, M -where the m -th sequence contains k frames- and apply a decomposition model D_w^C on input sequences T , and windowed frames X from T , e.g. in the generative process of speech production (θ_1) the long-term speaker identity variable S influences short-term phonetic content Z . The decomposed time series $\{t'^{(m)}, t'^{(m)}_1, \dots, t'^{(m)}_C\}$, $\{x'^{(k,m)}, x'^{(k,m)}_1, \dots, x'^{(k,m)}_C\}$ at the two distinct time scales T', X' are analyzed by different DecVAE branches ϕ_S, ϕ_Z to learn latent representations on subspaces $\{\tilde{s}_0^{(m)}, \tilde{s}_1^{(m)}, \dots, \tilde{s}_C^{(m)}\}$, $\{\tilde{z}_0^{(k,m)}, \tilde{z}_1^{(k,m)}, \dots, \tilde{z}_C^{(k,m)}\}$. DecVAE approximates the true prior distributions S, Z by disentangling inside the latent subspaces and then aggregating the subspaces through functions $h(\cdot), g(\cdot)$ to obtain \tilde{S}, \tilde{Z} (detailed in Methods).

Results

Method Overview

VDA leverages the DecVAE architecture to learn unsupervised deep representations with enhanced disentanglement and interpretability (Fig. 1d). The input to DecVAE consists of time series denoted by X , which are decomposed into C distinct components using a signal decomposition model \mathcal{D}_w^C . Each component captures localized time-frequency features, enabling the model to isolate spectral signatures that correspond to latent generative factors (Supplementary Fig. 2). This decomposition introduces a strong inductive bias, allowing DecVAE to approximate the true factors of variation within a structured latent space \tilde{Z} , where each subspace $\tilde{z}_c \in \tilde{Z}$ corresponds to a distinct component of the input (Fig. 1b). The generative assumption underlying VDA posits that the observed data $x \sim p(x)$ arises from multiple latent subspaces $z_c \sim q(z_c|x'_c)$, each tied to a decomposed input $x'_c \sim p(x'_c)$. DecVAE operationalizes this by encoding each x'_c into its corresponding \tilde{z}_c , a latent approximation of the true z_c , and enforces latent reconstruction on the subspaces $\tilde{z}_0, \tilde{z}_1, \dots, \tilde{z}_C$ through the SSL contrastive task (Fig. 1c,d). This structure enables the model to disentangle overlapping generative factors by aligning latent dimensions with time-localized frequency dynamics (Fig. 1b).

To promote disentanglement during training, DecVAE incorporates a self-supervised contrastive loss that enforces orthogonality among latent subspaces, ensures accurate reconstruction of each component, and approximates a Gaussian prior within each \tilde{z}_c (Fig. 1d). These mechanics—orthogonalization, chromagram-guided dynamics, and subspace-specific prior regularization—collectively define the disentanglement-promoting structure of VDA. Furthermore, DecVAE can accommodate multi-scale temporal dynamics, enabling the simultaneous learning of multiple latent representations when factors of variation operate across distinct time scales (e.g. X, T in Fig. 1d) (see details in *Methods* section).

Following pre-training, DecVAE functions as a mapping from input X to a disentangled representation \tilde{Z} , which can be evaluated across downstream tasks. We assess the utility of \tilde{Z} in domains such as speech recognition, dysarthria severity estimation, and emotional speech classification. DecVAE supports both zero-shot and fine-tuned evaluation, allowing it to generalize to unseen tasks and incorporate new factors of variation—such as emotional state or clinical progression—without retraining. Additionally, latent response analysis provides interpretability by revealing how individual subspaces encode specific generative factors (see details in the *Applications* section).

Simulated speech data

We first test DecVAE on the SimVowels simulated speech dataset (see 'Datasets'). The SimVowels data represents a generative speech process with two exclusively frequency-related factors, the phonetic content (vowel) and the speaker identity encoded into the three formants that generate each vowel (Supplementary Fig. 4). We observe that DecVAE models are able to disentangle frequency components in the frame Z (Fig. 2c) and sequence S (Fig. 2d) latent spaces. Using the decomposition model $\mathcal{D}_w^C, C = 3$ on the input X acts as a good starting point for disentanglement (Fig. 2a,b). DecVAE's optimization through DELBO (see 'Variational decomposition autoencoding') further promotes this structure resulting in smooth, well-separated frequency embeddings (Supplementary Fig. 5). Consequently, DecVAE can successfully approximate the prior $p(z)$ in both frame and sequence branches (Fig. 2a,b), leading to enhanced disentanglement performance for vowels (Fig. 2c, middle) and speakers (Fig. 2d, middle), compared to a VAE model without frequency sensitivity (Fig. 2c,d, right). DecVAE constructs an elaborated latent space shaped by decomposition orthogonality, reconstruction and the prior approximation (Fig. 2e),

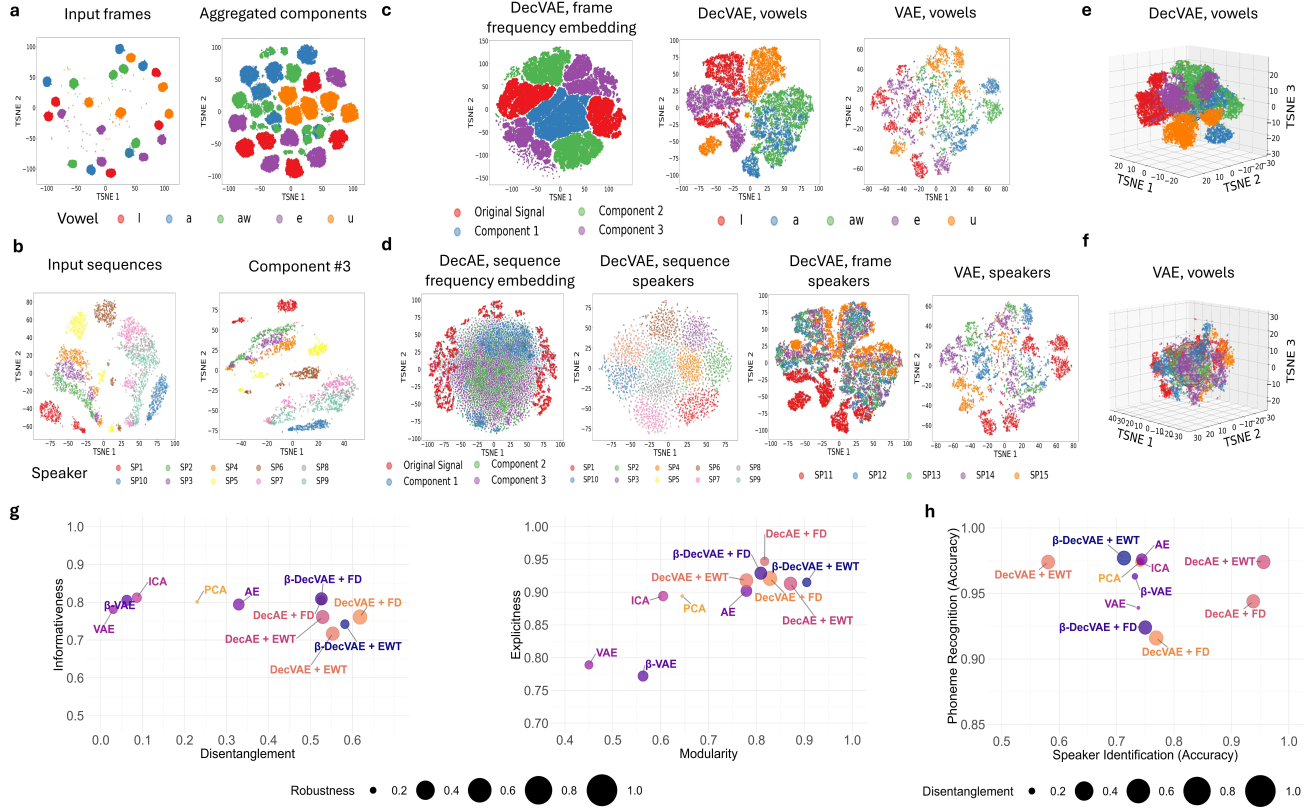


Fig. 2 | Simulated speech data (SimVowels). **a**, TSNE [21] of development set frame-level vowel-colored inputs, (left): Mel filterbank features of original signal, (right): decomposed Mel filterbank features of the original and components signals, after aggregation. **b**, TSNE of training set sequence-level speaker-colored inputs, (left): Mel filterbank features of original signal, (right): decomposed Mel filterbank features of the third component, after aggregation. **c**, TSNE of latent spaces using **a** as inputs (left) DecVAE with empirical wavelet transform (EWT) [22] frequency-resonant frame embedding, (middle) DecVAE with EWT [22] vowel-colored embedding, (right) VAE [10] vowel-colored embedding. **d**, TSNE of latent spaces using **a,b** as inputs, (left) DecVAE with EWT frequency-resonant sequence embedding, (mid-left) DecVAE with EWT [22] speaker-colored sequence embedding, (mid-right) DecVAE with EWT [22] speaker-colored frame embedding, (right) VAE [10] speaker-colored frame embedding. **e**, TSNE projection of DecVAE with EWT [22] vowel-colored latent space (two batches) along with a multivariate Gaussian distribution (sphere). **f**, TSNE projection of VAE [10] vowel-colored latent space (two batches) along with a multivariate Gaussian distribution (sphere). **g**, (left) disentanglement (x-axis) versus informativeness (y-axis) from DCI [23] and robustness (circle size), (right) modularity (x-axis) versus explicitness (y-axis) [24] and robustness [25] (circle size). **h**, speaker identification (x-axis) versus phoneme (vowel) recognition (y-axis) and disentanglement [23] (circle size) performance of β -DecVAE variants and state-of-the-art methods VAE [10], β -VAE [18], ICA [26], PCA [27] ($\beta = 0.1$).

compared to the weaker structural bias of only prior approximation in VAE-based models (Fig. 2f) and other supporting methods (Supplementary Fig. 6).

To quantify disentanglement quality, we utilize several disentanglement metrics (see ‘Performance Evaluation’) to measure the representation properties of disentanglement, informativeness and total correlation. DecVAE representations are more disentangled and more informative according to two measurement frameworks, DCI [23] (Fig. 2g, left) and modularity-explicitness [24] (Fig. 2g, right) outperforming VAE-based models and dimensionality reduction methods ICA and PCA (details and ablations in Supplementary Table 6). DecVAE representations are robust to perturbations [25], with higher IRS robustness (Fig. 2g). The enhanced disentanglement performance of DecVAE models is translated into better task-related generalization in both vowel recognition and speaker identification accuracies (Fig. 2h, Supplementary Tables 7,8). We also examine the learned representations under a Gaussian total correlation and mutual information between dimensions perspective, with unsupervised metrics

GCN [28] and MI. DecVAE models achieve very low MI and GCN scores slightly behind other methods despite the residuals of shared information that might exist in the aggregated latent in the components and original signal (Supplementary Fig. 7a, Supplementary Table 6).

Moreover, we examine the importance of the choice of decomposition model D_w^C by comparing our custom-made filter decomposition (FD) with three different state-of-the-art methods, empirical mode decomposition (EMD) [29], variational mode decomposition (VMD) [30], EWT [22]. We find out that the choice of decomposition is very important for a frequency-resonant embedding that translates into good task-related performance (Supplementary Fig. 5,8). The decomposition should successfully recover frequency-related events that are orthogonal and assign them to the correct component without mode mixing, i.e., information shared between different components. FD and EWT provide the best performance due to the nature of filters and wavelet transform that promotes time-frequency orthogonality, resulting to less correlated components in the input domain (Supplementary Fig. 9). In VMD and EMD, input correlations propagate to the latent space and contaminate the generative factors separation (Supplementary 8). This is naturally translated into worse performance in disentanglement and task-related metrics (Supplementary Tables 6,7,8). Knowing that SimVowels has three generative subspaces that correspond to the three formants that generate a vowel, we use a number of components $C = 3$; increasing to $C = 4$ has minor improvements, possibly due to slightly improved information allocation across components (Supplementary Fig. 10).

We also examine the β parameter that controls the prior approximation pressure in DELBO (Supplementary Fig. 11); β -DecVAE models demonstrate a compression of their latent space as the value of β increases, an effect that has been documented in β -VAEs [18], which may though have a harmful effect on disentanglement. Indeed, although β -DecVAE models are more robust to the choice of β compared to β -VAE models, due to the additional disentanglement dynamics, we observe a general decline in all metrics as β increases, with better performance in the low β range (0,1,1) (Supplementary Fig. 12).

Disentanglement of real speech data

We apply DecVAE on real speech to disentangle phoneme from speaker identity in the TIMIT [31] dataset (Fig. 3). We note that DecVAE extends the capability of learning a frequency-resonant embedding to real speech that contains other phonetic content beside vowels (Fig. 3b, Supplementary Fig. 5). The decomposition model $D_w^C, C = 4$ provides a more separated input space for phonemes (Fig. 3a) and speakers (Fig. 3b). DecVAE learns smoother representations where phonemes (Fig. 3c) and speakers (Fig. 3d) are more disentangled, and with a more Gaussian latent distribution (Fig. 3e) compared to VAE-based models [10, 18] (Fig. 3f). Although all methods manage to recover an embedding where phonemes are well separated, DecVAEs demonstrate more aptitude in creating representations where both generative factors can be separated (Supplementary Fig. 13).

In terms of disentanglement quality, DecVAE models with EWT [22] and FD display higher disentanglement, informativeness, robustness and explicitness, but reduced modularity compared to other methods (Fig. 3g). PCA, ICA and VAE-based models have slightly less correlated latent dimensions than DecVAEs due to the residual correlations between input components in DecVAEs (Supplementary Fig. 7b). Overall, DecVAE models learn more informative representations for the task of speech recognition (higher informativeness and explicitness), are more disentangled, and can encode relations between generative factors and latents more robustly, compared to other methods (Fig. 3h, Supplementary Table9). β -VAE [18] needs less dimensions to encode speech data (higher completeness) (Fig. 3h, Supplementary Table9). PCA [27] learns the most uncorrelated latent space that is though

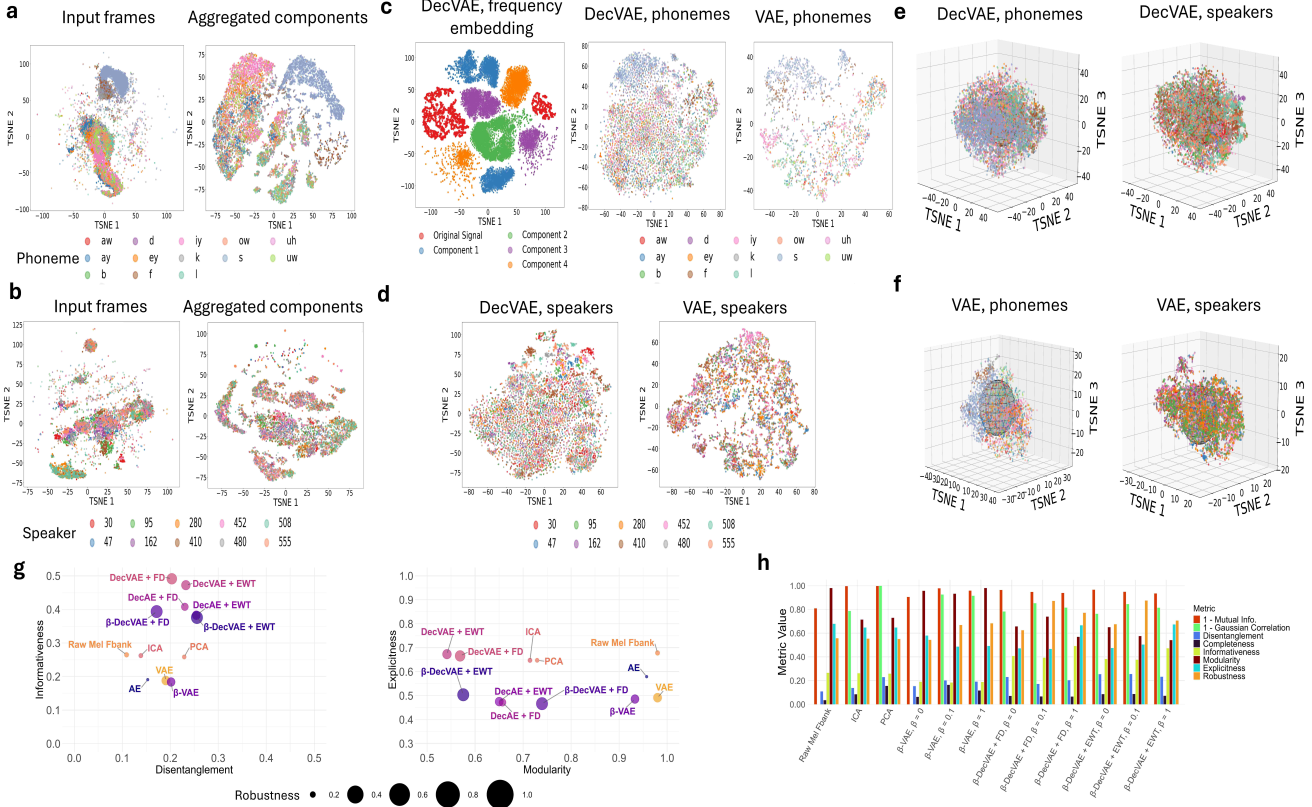


Fig. 3 | Real speech data TIMIT [31]. **a**, TSNE [21] of a subset (13 phonemes from 6 batches) of the development set, frame-level phoneme-colored inputs, (left): Mel filterbank features of original signal, (right): decomposed Mel filterbank features of the original and components signals, after aggregation. **b**, TSNE of a subset (10 speakers from 6 batches) of the development set, (left): Mel filterbank features of original signal, (right): decomposed Mel filterbank features of the third component, after aggregation. **c**, TSNE of latent spaces using **a** as inputs (6 batches) (left) DecVAE with EWT [22] frequency-resonant frame embedding ($C = 4$), (middle) DecVAE with EWT [22] phoneme-colored embedding, (right) VAE [10] phoneme-colored embedding. **d**, TSNE of latent spaces using **a,b** as inputs (6 batches), (left) DecVAE with EWT [22] frequency-resonant embedding, (mid-left) DecVAE with EWT [22] speaker-colored embedding, (mid-right) DecVAE with EWT [22] speaker-colored frame embedding, (right) VAE [10] speaker-colored frame embedding. **e**, TSNE projection of DecVAE with EWT [22] phoneme-colored latent space (6 batches) along with a multivariate Gaussian distribution (sphere). **f**, TSNE projection of VAE [10] phoneme-colored latent space (6 batches) along with a multivariate Gaussian distribution (sphere). **g**, (left) disentanglement (x-axis) versus informativeness (y-axis) from DCI [23] and robustness [25] (circle size), (right) modularity (x-axis) versus explicitness (y-axis) [24] and robustness [25] (circle size). **h**, total disentanglement performance of β -DecVAE variants and state-of-the-art methods VAE [10], β -VAE [18], ICA [26], PCA [27].

not disentangled in terms of generative factors, whereas the raw Mel filterbank inputs are already quite informative for the speech recognition task [16, 17] (Supplementary Table9).

Increasing the number of components C has a beneficial effect on all disentanglement metrics (Supplementary Fig. 14c) as real speech has more complex, albeit similar, spectral structures to our simulations since consonants do not abide to a clear formant-based generation process like vowels [32] (Supplementary Fig. 4). Similarly, we note that β -VAE models rely only on the structural bias of Gaussian prior approximation, whereas DecVAEs can disentangle even when $\beta = 0$ (Supplementary Fig. 14a). We find that as in simulations, the optimal $\beta = 0.1$ brings an increase in all metrics (Supplementary Fig. 14a).

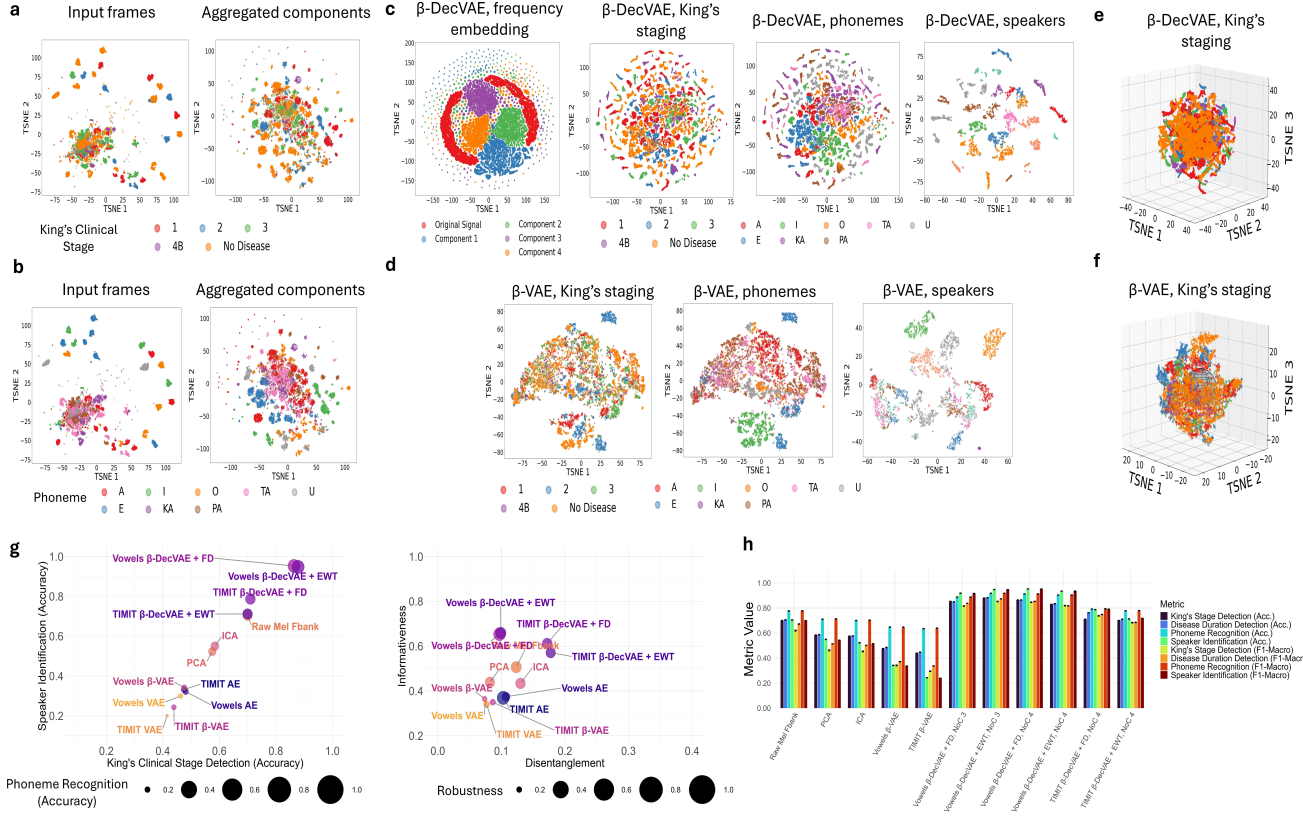
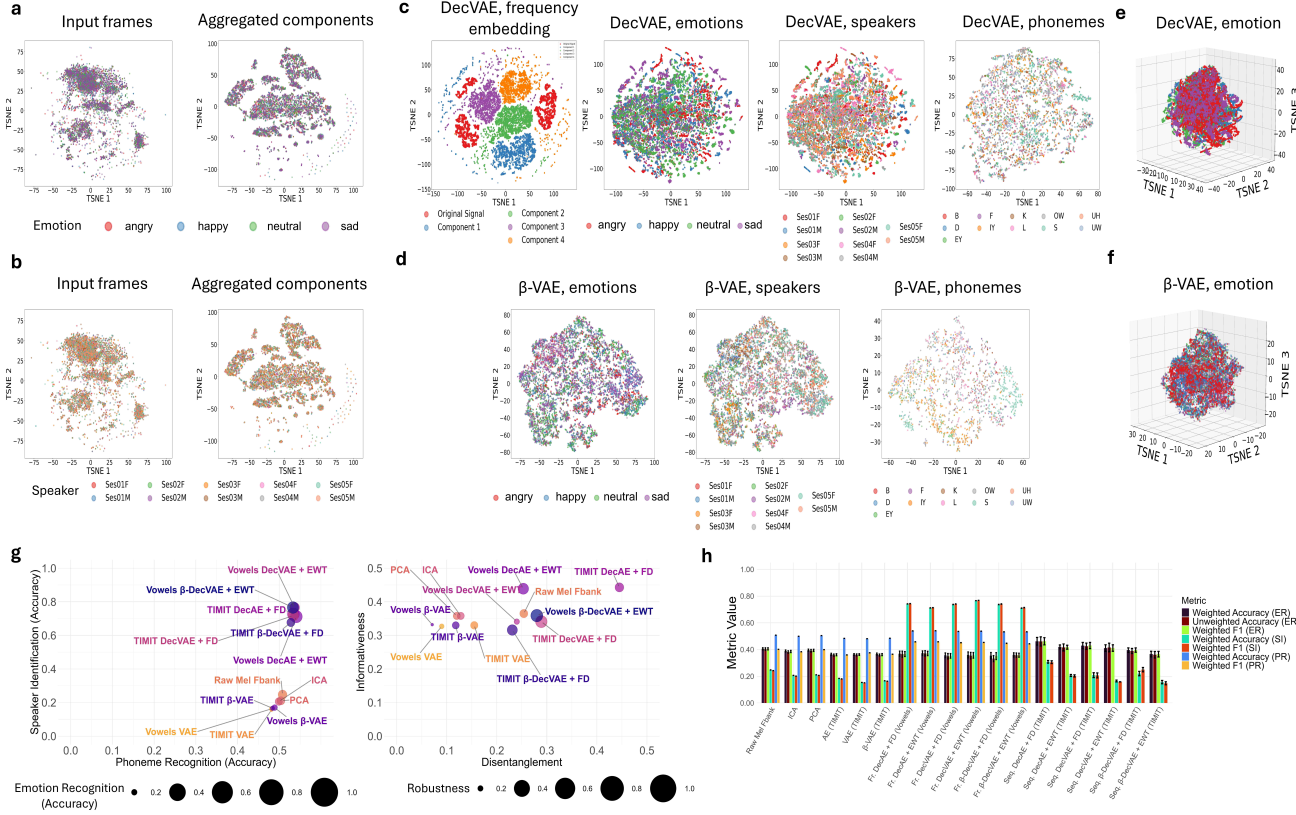


Fig. 4 | Zero-shot disentanglement on dysarthric speech data VOC-ALS [3]. **a**, t-SNE [21] of a subset (4 batches) of the dataset, frame-level King's clinical stage [33]-colored inputs, (left): Mel filterbank features of original signal, (right): decomposed Mel filterbank features of the original and components signals, after aggregation. **b**, t-SNE of a subset (4 batches) of the dataset, frame-level phoneme-colored inputs (left): Mel filterbank features of original signal, (right): decomposed Mel filterbank features of the third component, after aggregation. **c**, t-SNE of latent spaces using **a** as inputs and a pre-trained β -DecVAE on SimVowels ($\beta = 0.1$) for zero-shot evaluation (4 batches) (left) β -DecVAE with FD, frequency-resonant frame embedding ($C = 4$), (middle-left) β -DecVAE with FD, King's clinical stage [33]-colored embedding, (middle-right) β -DecVAE phoneme-colored embedding, (right) β -DecVAE speaker-colored embedding (for 10 speakers). **d**, t-SNE of latent spaces using **b** as inputs and a pre-trained on SimVowels β -VAE ($\beta = 0.1$) for zero-shot evaluation (4 batches), (left) β -VAE [18] King's clinical stage [33]-colored embedding, (mid-right) β -VAE [18] phoneme-colored embedding, (right) β -VAE [18] speaker-colored embedding (for 10 speakers). **e**, t-SNE projection of β -DecVAE with FD, King's clinical stage [33]-colored latent space (4 batches) along with a multivariate Gaussian distribution (sphere). **f**, t-SNE projection of β -VAE [18] King's clinical stage [33]-colored latent space (4 batches) along with a multivariate Gaussian distribution (sphere). **g**, (left) King's clinical stage [33] detection (x-axis) versus speaker identification (y-axis) and phoneme recognition (circle size), (right) disentanglement (x-axis) versus informativeness (y-axis) from DCI [23] and robustness [25] (circle size). **h**, total classification performance (accuracies and F1-macro with 95% confidence intervals error bars) of β -DecVAE variants and state-of-the-art methods VAE [10], β -VAE [18], ICA [26], PCA [27], in predicting King's clinical stage, disease duration, phoneme recognition, speaker identification.

Zero-shot disentanglement of dysarthria severity from speech factors

To further test the capacity of DecVAE to disentangle more challenging biomedical data, we apply DecVAE as a zero-shot transfer learned module without any adaptation on dysarthric speech data [3] where we assume three generative factors, phoneme, speaker identity and amyotrophic lateral sclerosis (ALS) progression. Dysarthric speech mainly manifests through an altered fundamental frequency f_0 , which alters the entirety of the speech spectrum [3]. β -DecVAEs retain the frequency-resonant structure of the latent space even on unseen data distributions, and demonstrate great success in disentangling three generative factors in the data and creating interpretable embeddings that reflect this disentanglement (Fig. 4c). Compared to DecVAEs, VAE-based models and other methods fail to separate all three factors in the latent space (Fig. 4d, Supplementary Fig. 15). The strong structural biases of β -



DecVAE allow disentanglement of more complex processes compared to healthy speech, providing an interpretable latent structure that cannot be learned with the prior approximation only (Fig. 4c,d,e,f).

DecVAEs demonstrate strong performance in all disentanglement and task-specific evaluations with increased generalization in all generative factors classification (Fig. 4h), with more disentangled, informative and robust representations (Fig. 4g). PCA [27] and ICA [26] learn the most uncorrelated latent spaces in terms of MI and GCN (Supplementary Table10), however DecVAEs display uncorrelated latents comparable to VAEs (Supplementary Fig. 7c). Notably DecVAEs significantly outperform other methods in all other disentanglement and task-specific metrics except completeness (Supplementary Tables10,11).

Fine-tuning disentanglement on emotional speech data

To test VDA in an even more challenging task, we apply DecVAEs on emotional speech data from IEMOCAP [34] in a transfer learning and fine-tuning scheme. As there is no direct correspondence of emotion in the time-frequency domain, this is an even more challenging task with three generative factors of emotion, phoneme and speaker. The input data and their decomposition does not offer any separation for emotion or phonetic content (Fig. 5a,b). DecVAE can adapt to the new data distribution and learns a frequency-resonant embedding (Fig. 5c), which leads to an enhanced emotion, speaker and phoneme disentanglement (Fig. 5c), compared to other state-of-the-art disentanglement methods such as β -VAE (Fig. 5d, Supplementary Fig. 16). DecVAE variants significantly outperform other methods in generalizing over speaker identification, phoneme recognition and emotion recognition (Fig. 5g,h) as well as disentanglement quality performance with increased disentanglement, informativeness and robustness (Fig. 5g, Supplementary Fig. 17). DecVAEs utilize information from both time scales (frame and sequence) to increase their performance in emotion detection through the sequence branch (Fig. 5h). Notably, DecVAE models outperform other methods on all disentanglement metrics except modularity, MI, and GCN, where PCA and ICA learn the most uncorrelated latent spaces (Supplementary Table 12, Supplementary Fig. 7d).

Interpretability of disentangled latent spaces

To shed light upon the way DecVAEs encode and disentangle information in their latent spaces, we perform a latent traversal analysis; due to the absence of a decoder in our implementations, we visualize the latent space responses in changes of the input generative factors (see 'Applications'). In our simulations, we compare β -VAEs with our DecVAEs and various decomposition methods (Supplementary Fig. 18). The choice of decomposition affects how well can DecVAE encode different vowel and speaker combinations in each latent space. We see that DecVAE splits the information across the different latent subspaces of oscillatory components, allowing for a more efficient allocation of information (Supplementary Fig. 18), whereas VAE models compress all the information in a few dimensions (higher compactness). We observe similar latent patterns for real speech data (Fig. 6a, Supplementary Fig. 19); the enhanced disentanglement of DecVAEs is even more prominent here, with VAEs and β -VAEs being not able to learn a separable representation for speakers and phonemes. We also notice greater separability in some components than others.

Similarly, the zero-shot evaluation on dysarthric speech shows that DecVAE can efficiently allocate information in different subspaces to create disentangled and separable embeddings for three generative factors (Fig. 6b, Supplementary Fig. 20). Since King's clinical staging reflects a fixed classification of disease severity for each individual [33], we treat it as a static reference point and focus our visualization on how phonetic content varies across these clinical stages. This approach allows us to explore how specific acoustic or articulatory features align with progressive motor decline, without implying intra-speaker variability over time.

In the emotional speech case where we have three varying factors, we isolate emotions and visualize the contour of the most informative latent dimension for the phoneme-speaker response (Fig. 6c, Supplementary Fig. 21). DecVAEs again allocate information in a complementary fashion, with each oscillatory component latent subspace covering different ranges of the generative factors' values. β -VAEs on the other hand, encode information by using a single latent space, thus being limited in the encoding optimization that they can achieve (Fig. 6c last column).

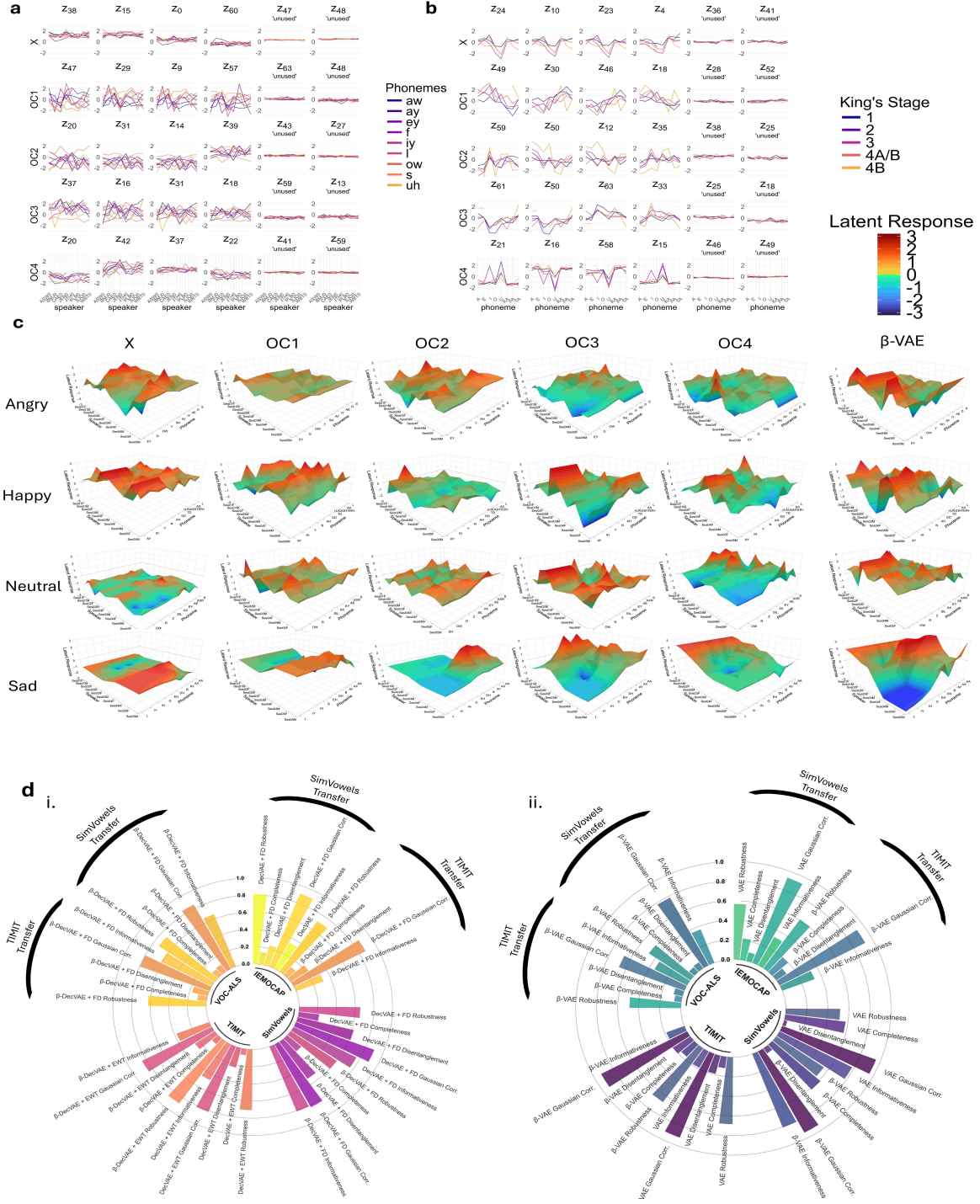


Fig. 6 | Latent response interpretability analysis and overall performance. **a**, latent traversals on TIMIT [31] for the DecVAE + EWT model by keeping the speaker variable fixed and traversing the phoneme variable. **b**, latent traversals on VOC-ALS [3] for the β -DecVAE ($\beta = 0.1$) + EWT model by keeping the phoneme variable fixed and traversing the King's clinical stage. **c**, latent traversals on IEMOCAP [34] for the DecVAE + EWT (first five columns) and β -VAE ($\beta = 0.1$), both transferred from TIMIT [31] model by keeping the emotion variable fixed and traversing the phoneme-speaker plane. **d**, overall disentanglement performance of (i) β -DecVAE and (ii) β -VAE models, across all utilized datasets; DecVAEs demonstrate generalization capabilities in disentanglement performance across all utilized metrics and tasks in the four datasets.

Discussion

Variational decomposition autoencoding is a novel disentangled representation learning framework for complex, nonstationary, high dimensional time series data with multiple generative factors. DecVAE facilitates disentanglement through the synergy of decomposition and prior approximation mechanics in disentangling frequency-related factors inside latent subspaces (Fig. 1c). VDA is applicable to different time scales beyond the short-term phonetic content (Fig. 1d); a second sequence-level latent proves to be quite useful as a natural disentanglement mechanism to isolate slow variables and brings performance improvements in the cases of SimVowels and IEMOCAP [34] (Fig. 2,5, Supplementary Tables 13,7,8).

We evaluated DecVAE using a wide variety of disentanglement and task-specific metrics (see 'Performance Evaluation'). A domain where DecVAE consistently underperformed compared to other methods is compactness of representations, measured by DCI completeness [23]. In VAEs compactness is enforced as an effect of the combined Gaussian prior approximation and the decoder reconstruction that embeds similar samples close to each other in the latent space. We observe the effects of having a compact but entangled and uninformative representation in the latent traversals analysis of VAE models, whereas DecVAE representations are not compact but they are disentangled and informative (Fig. 6a,b,c, Supplementary Fig. 18,19,20,21).

Our experiments demonstrated the capacity and flexibility of DecVAEs as foundational deep disentanglers through superior performance in four datasets (Fig. 6d). DecVAE is a self-supervised model that undergoes a pre-training phase; after pre-training it can be transferred as a representation function that maps high-dimensional data to low-dimensional disentangled representations. We have evaluated DecVAE with very simple classifiers in the post-training phase to exemplify the quality of the learned representations. We demonstrated how once pre-trained, DecVAE can be used as a zero-shot or fine-tuned disentangler to generalize to unseen generative factors from different domains, a capacity that state-of-the-art methods did not have. Moreover, despite its simple architecture as a convolutional encoder and the absence of a decoder, DecVAE manifested significant generalization ability in performing well on all task-specific evaluations across different datasets.

Our ablations on DecVAEs reveal that disentanglement arises even without the Gaussian prior approximation (Supplementary Fig. 22a,b). This happens because DecVAE consistently maximizes and minimizes divergences of components to other components and original signal in real and simulated data (Supplementary Fig. 22,Supplementary Fig. 24). The choices of important hyperparameters such as β (Supplementary Fig. 22a,b,c,d), decomposition method (Supplementary Fig. 22e,f), components number (Supplementary Fig. 23e,f), aggregation function $g(\cdot)$ (Supplementary Fig. 26e,f) dictate the exact structural bias of VDA. Balance between noisy, redundant representations and structural biases is key to performance of DecVAEs. When the optimization problem becomes too demanding, such as when using a large number of components C (Supplementary Fig. 10), convergence slows down. Similarly, using very few frames in the SSL loss calculation (Supplementary Fig. 10a,b, 14b) also hinders learning. The same applies when the input is more abstract, such as raw waveform instead of Mel filterbanks (Supplementary Fig. 22d). These conditions can negatively impact both disentanglement and informativeness of the learned representations. This is consistently observed across our ablation results (Supplementary Tables 6, 7, 8).

Disentanglement Through Structured Latent Decomposition

We have in purpose excluded the decoder network from our analysis to showcase the strength of our structural biases. The decoder is an essential part of disentanglement in VAE-based methods; yet, aligned with recent theo-

retical advances in the understanding of VAEs [15][11], our work posits that enforcing structural biases is actually what mostly promotes disentanglement. Our results showcase that decomposition can generalize disentanglement by accounting for more latent interactions besides the orthogonal Gaussian latent structure [18, 19, 20]. We provide an intuition on why this happens in Supplementary Information6. More specifically, our analysis shows that VDA is a hybrid of variational methods and PCA-based methods. In Supplementary Information7 we analyze how VDA, similarly to PCA, pursues orthogonal components directions, and variationally so, similarly to VAEs. In contrast to VAEs where this happens coincidentally by approximating an uncorrelated latent structure, in DecVAEs we explicitly insert the decomposition bias and learn a latent space where the representation is aligned according to time-frequency related properties; this allows us to formulate DecVAE as a singular value decomposition (SVD) operation on the input (Supplementary Fig. 1).

Design insights and extension pathways of variational decomposition autoencoding

We showcased the versatility of DecVAEs in disentangling various generative processes in speech data using minimal data preprocessing or modality assumptions. We implemented DecVAEs as deep encoders with one-dimensional convolution layers; this makes them suitable for processing any sequence modality and allows applications in a multitude of scientific domains. Our applications tackled a highly challenging and complex time series modality—audio—demonstrating exceptional performance. We focused our evaluation on disentanglement quality and not generation; disentanglement is an important prerequisite for high quality generation, an important task that we leave as future work. The VDA dynamics of orthogonality and reconstruction implemented through a self-supervised contrastive task, allow the potential extension of our method to disentangle multi-modal datasets by using modalities as components instead of utilizing a decomposition. In such settings, each modality—be it audio, visual, textual, or physiological—can be treated as a distinct input channel with its own time-frequency or spatial signature, enabling DecVAE to learn modality-specific latent subspaces while preserving cross-modal coherence. This formulation naturally accommodates fusion tasks, where disentangling modality-specific generative factors is critical for downstream interpretability, such as in emotion recognition from audiovisual data, clinical decision support from speech and biosignals, or scene understanding from video and text. By aligning latent dimensions with modality-driven structure rather than decomposed frequency bands, DecVAE can generalize its disentanglement mechanics to heterogeneous data sources, offering a unified framework for structured representation learning across domains.

While the proposed framework demonstrates broad applicability, several aspects invite further exploration. The performance of DecVAE is influenced by the choice of decomposition method, as certain techniques may introduce residual correlations that affect latent separation. To address this, we systematically evaluated multiple decomposition strategies and selected those that promote frequency-resonant orthogonality. Additionally, the current architecture is optimized for sequential data, which may require structural adaptation for spatial modalities such as images. Our encoder-only design also prioritizes representation quality over generative synthesis, leaving decoder integration as a promising direction for future work. Finally, while contrastive regularization and orthogonality constraints help mitigate latent overlap, further refinement may enhance modularity and independence in complex, multi-modal settings. These considerations highlight the flexibility of the VDA framework and suggest clear pathways for extension across data types and application domains.

Building on the novel optimization objective of VDA, future work could further explore its extension to non-sequential data domains, such as images, by adapting the DecVAE architecture to accommodate spatial rather than

temporal decomposition. This would involve restructuring the encoder to capture localized spatial features and redefining the decomposition model to reflect image-specific priors. Additionally, the contrastive self-supervision and orthogonality constraints could be repurposed to enforce semantic separation across modalities in multi-modal datasets. Treating each modality as a distinct latent subspace may enhance robustness to missing inputs, domain shifts, and modality-specific noise, paving the way for interpretable, disentangled representations in heterogeneous data environments. Taken together, these insights affirm that VDA is not merely a refinement of existing latent modeling techniques—it is a principled, domain-agnostic framework for disentangling structure in dynamic data, poised to advance interpretability, generalization, and scientific discovery across modalities.

Methods

Figure 1 displays the main working principles of variational decomposition autoencoding (VDA) and its neural network implementation of Decomposition Variational Autoencoder (DecVAE) (Supplementary Fig. 2). DecVAE accepts sequences from a dataset $X = \{x_1, x_2, \dots, x_N\} \in \mathbb{R}^{N \times L}$ and applies a decomposition module \mathcal{D}_w^C to decompose the input sequence x_m into a series of components (Supplementary Fig. 2). The DecVAE encoder then receives the inputs and their components and embeds them in latent subspaces $\{\tilde{z}^0, \tilde{z}^1, \dots, \tilde{z}^C\}$, according to their distinct time and frequency domain characteristics. An aggregation function $g(\cdot)$ then projects the collection of latent subspaces onto the latent space \tilde{Z} . In our ablations we find that the best choice of aggregator is a simple concatenation of subspaces contrary to more complex aggregations such as learnable projection (see ‘Aggregation of latent subspaces’). Fig. 1d shows how DecVAE can also simultaneously handle latent variables in different time scales (see ‘Multiple latent variables’).

In contrast to variational autoencoding [10, 18] (Fig. 1a, Supplementary Table 2), VDA (Fig. 1b) assumes generative subfactors that are characterized by prior distributions $p(z_1), p(z_2), \dots, p(z_c)$. The generative factors are then generated by superposing information from these subspaces. Whereas VAEs operate to directly recover the true distribution of generative factors $p(z)$, DecVAEs recover the sub-factor distributions that synthesize $p(z)$. As in VAEs, there is a single inference model q_ϕ that approximates the prior distribution of each latent subspace. Starting from the input space X and observed data distributions $p_D(x), p_D(x_1), p_D(x_2), \dots, p_D(x_C)$ after the decomposition model \mathcal{D}_w^C has been applied, DecVAE can project data to a latent space where the approximation $q_\phi(z|x)$ of the true posterior can be estimated.

Figure 1c illustrates the disentanglement mechanics employed in VDA; VDA is an enhanced variational inference scheme that complements the Gaussian prior approximation of VAEs, with two disentanglement forces from the input decomposition domain, orthogonality and reconstruction. During the training of DecVAEs, the dynamics between the latent subspaces of components and the original signal, as well as the Gaussian prior approximation, lead to an equilibrium in the latent approximation space \tilde{Z} that leads to disentangled representations. This optimization objective which we term variational decomposition evidence lower bound (DELBO) is expressed as follows:

$$\mathcal{L}_{DELBO}(\phi; X, Z) = L_{recon} - L_{ortho} - \beta L_{prior} \quad (1)$$

The decomposition dynamics of reconstruction and orthogonality are enforced in the latent space through the terms L_{recon} and L_{ortho} . L_{recon} maximizes the similarity of individual component latent subspaces z_i to the latent subspace of the original signal z , by encouraging the Jensen-Shannon divergence (JSD) [35] of pairwise

distributions $\{z_i, z\}$ to approach zero. L_{ortho} enforces orthogonality between all pairs of components so that $z_i \perp z_j = 0, \forall i \neq j$, by encouraging pairwise distribution to diverge to a JSD of one.

The importance of L_{recon} and L_{ortho} is critical for the disentanglement of the latent space (Supplementary Fig. 22a, upper left and right panels). Even in the absence of a Gaussian prior pressure ($\beta = 0$), these terms converge to respect the input decomposition dynamics. L_{prior} is responsible for enforcing the multivariate Gaussian distribution on all latent subspaces $\{z, z_1, z_2, \dots, z_C\}$ with a user-defined pressure β [18], contributing towards continuity of the subspaces and the final latent space Z . Increasing the value of β (Supplementary Fig. 22a), results in a slower convergence of the objective as an additional term is added, and also influences the convergence of the decomposition terms L_{recon}, L_{ortho} . The effect of L_{prior} is more pronounced in the early stages of training and its convergence is fast (Supplementary Fig. 22a, lower right panel). Moreover, a high value of β can be detrimental to the training as it can significantly slow down convergence of the other two terms (Supplementary Fig. 22a,b, upper panels).

Problem formulation

We consider N i.i.d. observations of a dataset $X = \{x_1, x_2, \dots, x_N\}$ and we assume that each observation is generated by a three-step process (Fig. 1.b.i), which involves an unobserved continuous latent variable z , and a set of latent variables z_1, z_2, \dots, z_C that are parts or components of z . Components are characterized by orthogonality with respect to each other (Eq. (2)) and their superposition satisfies the reconstruction principle and yields z in a latent space of generative factors Z (Eq. (3)):

$$\langle z_i, z_j \rangle = \sum_{i,j}^C z_i z_j^* = 0, \forall i \neq j \quad (2)$$

$$z = \sum_i^C z_i \quad (3)$$

where $\langle \cdot, \cdot \rangle$ is defined as the dot product in the space Z and $(*)$ denotes the complex conjugate. For a single observation x_n the three-step generative process θ generates components $z_{n1}, z_{n2}, \dots, z_{nC}$ from prior distributions $p(z_1), p(z_2), \dots, p(z_C)$, which precede and compose the unobserved value z_n that follows a prior distribution $p(z)$. Subsequently, x_n is generated by conditional distribution $p_\theta(x|z_1, z_2, \dots, z_C) \equiv p_\theta(x|z)$. The parameters of the process θ and the values of the set of latent variables $\{z_n; z_{n1}, z_{n2}, \dots, z_{nC}\}$ are unknown and we want to estimate them. The joint probability for this three-step generative process is given by Eq. (4):

$$p_\theta(X, Z_1, Z_2, \dots, Z_C) = \prod_{n=1}^N p_\theta(x_n|z_1^n, z_2^n, \dots, z_C^n) p_\theta(z_1^n) p_\theta(z_2^n) \cdots p_\theta(z_C^n) \quad (4a)$$

$$p_\theta(z^n) = p_\theta(z_1^n) p_\theta(z_2^n) \cdots p_\theta(z_C^n) \quad (4b)$$

$$p_\theta(x_n|z^n) = p_\theta(x_n|z_1^n, z_2^n, \dots, z_C^n) \quad (4c)$$

Each term of the joint probability in Eq. (4) can be expressed as:

$$p_\theta(x|z_1, z_2, \dots, z_C) = \mathcal{N}(x|0, diag(z_1, z_2, \dots, z_C))$$

$$p_\theta(z_i) = \mathcal{N}(z_i|0, \sigma_{z_i}^2 I), \forall i \in 1, \dots, C$$

where θ parameterizes the generative process, and the priors $p_\theta(z_i)$ that we assume here over the latent variables z_i are isotropic multivariate Gaussian distributions centered around 0. The conditional distribution of observed x is a multivariate isotropic Gaussian with a diagonal covariance matrix that represents the orthogonality property of latent variables z_i , as in Eq. (2).

Moreover, as also is the case in the variational autoencoding framework [10], the true posterior distribution $p_\theta(z|x)$ is intractable, and an inference model $q_\phi(z|x)$ is needed to approximate the true posterior:

$$q_\phi(Z|X) = \prod_{n=1}^N q_\phi(z_1^n|x_n, z_2^n, \dots, z_C^n) q_\phi(z_2^n|x_n, z_1^n, z_3^n, \dots, z_C^n) \cdots q_\phi(z_C^n|x_n, z_1^n, z_2^n, \dots, z_{C-1}^n) \quad (5)$$

Each term of the posterior in Eq. (5) can be expressed as:

$$\begin{aligned} q_\phi(z_1|x, z_2, z_3, \dots, z_C) &= \mathcal{N}(z_1|f_{\mu_{z_1}}(x, z_2, z_3, \dots, z_C), f_{\sigma_{z_1}^2}(x, z_2, z_3, \dots, z_C)) \\ q_\phi(z_2|x, z_1, z_3, \dots, z_C) &= \mathcal{N}(z_2|f_{\mu_{z_2}}(x, z_1, z_3, \dots, z_C), f_{\sigma_{z_2}^2}(x, z_1, z_3, \dots, z_C)) \\ &\dots \\ q_\phi(z_C|x, z_1, \dots, z_{C-1}) &= \mathcal{N}(z_C|f_{\mu_{z_C}}(x, z_1, \dots, z_{C-1}), f_{\sigma_{z_C}^2}(x, z_1, \dots, z_{C-1})) \end{aligned}$$

where all the posteriors are isotropic multivariate Gaussian distributions. In practice, all functions $f_{\mu_{z_i}}, f_{\sigma_{z_i}^2}$ are neural networks and are parameterized jointly with the set of parameters ϕ . However, the factorization of the generative model in Eq. (4) does not constrain latent variables z_i to satisfy the reconstruction property of Eq. 3 and would either require multiple inference models, one for every latent variable, or hierarchical relations between the latent variables, such as $q_\phi(z_i|x, z_j)$, but not $q_\phi(z_j|x, z_i)$, for $i \neq j$, as the case is in Eq. (5), or as is done in [16].

Self-supervised latent decomposition

To address these challenges, the inference model of Eq. (5) is enhanced with a strong inductive bias of a decomposition model \mathcal{D}_w parameterized by w . The decomposition model can operate in the observed input domain X as a front-end to the inference model q_ϕ , or can be a part of the inference model q_ϕ and operate directly on the estimated latent space Z or any intermediate space H . Here we present variational decomposition autoencoding with the former approach.

We define a decomposition model \mathcal{D}_w^C as an iterative optimization algorithm with a stopping criterion over C iterations, that is applied on input time series observations x_n of the dataset $X \in \mathbb{R}^{K \times N}$ and yields a set of components $\{x_n^{(1)}, x_n^{(2)}, \dots, x_n^{(C)}\}$. The number of components C is a hyperparameter and is selected based on prior knowledge on the generative problem at hand. The oscillatory components yielded by \mathcal{D}_w^C may have distinct time and frequency domain characteristics and their nature will depend on the inductive biases of the decomposition algorithm, but they must always satisfy the properties of orthogonality and reconstruction of Eq. (2) and Eq. (3). Yet, when real data processing is involved, these properties are satisfied in the domain where \mathcal{D}_w^C operates, in this case the input time and frequency domain X , and are not guaranteed to be satisfied in a new domain $H = f(X)$.

To address this, we design a self-supervised contrastive latent decomposition optimization algorithm that leverages the structural biases of orthogonality and reconstruction enforced by \mathcal{D}_w^C in the input domain X , and aims to retain these structural dynamics in subsequent latent spaces H . Specifically, the following contrastive objective is formulated and minimized:

$$\mathcal{L}_{SSLDec} = L_{recon} - L_{ortho} \quad (6)$$

where right-hand side terms are formulated as:

$$\begin{aligned} L_{recon} &= \sum_{i=1}^C D(h_i \parallel h) \\ L_{ortho} &= \sum_{i=1}^C \sum_{j=1}^C 1[i \neq j] D(h_i \parallel h_j) \\ h_i &= f(x^{(i)}), h = f(x) \end{aligned}$$

where D is a function that measures divergence between the distributions of components h_i and original signal h in a space H . Specifically, the L_{recon} term enforces similarity of all components to the original signal in H , and the L_{ortho} term enforces the orthogonality or dissimilarity between each pair of components in H . The combination of those two terms enforces the reconstruction and orthogonality properties. The formulation of \mathcal{L}_{SSLDec} in Eq. (6) denotes an adversarial objective with two competing terms, as an equilibrium between attracting and repelling forces between the components and the original signal is sought in the optimization problem.

In practice, a function D must be carefully chosen to avoid representation collapse that arises as a behavior of a neural network optimizer in seeking trivial solutions that can minimize a contrastive learning objective function in Eq. (6) [36]. To that end, we use the JSD and to stabilize the adversarial objective in Eq. (6) we calculate the following quantities:

$$\begin{aligned} L_{recon} &= \sum_{i=1}^C w_{pos}^i D_{KL}(D_{JS}(h_i, h) \parallel p) \\ &\quad , \text{ where } p(y) = \epsilon, \forall y \in \{1, \dots, d\}, H^{d \times N} \\ L_{ortho} &= \sum_{i=1}^C \sum_{j=i+1}^C w_{neg}^{(i,j)} D_{KL}(D_{JS}(h_i, h_j) \parallel n) \\ &\quad , \text{ where } n(y) = 1, \forall y \in \{1, \dots, d\}, H^{d \times N} \\ \mathcal{L}_{SSLDec} &= L_{recon} + L_{ortho} \end{aligned} \quad (7)$$

where $w_{pos}^i, w_{neg}^{(i,j)}$ are hyperparameters that regulate the weighting of divergences between components h_i and original signal h in latent space $H^{d \times N}$ with dimensionality d , D_{KL} is the Kullback-Leibler (KL) divergence, D_{JS} is the JSD, and p, n are uniform target distributions, and ϵ is an arbitrarily small positive constant. The reformulation of the adversarial objective in Eq. (7) stabilizes the adversarial objective by transforming the competing terms into quantities that should both be minimized. The complete derivation of Eq. (7) and the algorithm to train a neural network with this loss is given in Supplementary Information ‘Self-supervised contrastive decomposition loss derivation and algorithm’ and Supplementary Alg. 2.

Variational decomposition evidence lower bound

The structural bias induced by the decomposition model allows us to formulate a variational decomposition evidence lower bound for the inference model on the marginal likelihood of an observation x_n by incorporating the

decomposition mechanics as developed in the self-supervised decomposition objective from Eq. (6), Eq. (7). In this work, we show that we can restrict our DecVAE model to an inference-only model, and demonstrate enhanced disentanglement and recognition capabilities, and hence our modified variational decomposition evidence lower bound does not need a generative model to recover the posterior distribution. We derive the full DELBO by working with a latent generative model $r_\psi, Z \rightarrow H$, parameterized with $\psi \subset \phi$, that is connected to the latent reconstruction decomposition mechanism. The derivation of the DELBO is given in Supplementary Information ‘Derivation of variational decomposition evidence lower bound’. The final DELBO is:

$$\begin{aligned}\mathcal{L}_{DELBO}(\phi; x, z, w_{pos}, w_{neg}, \beta) &= \sum_i w_{pos}^{(i)} \mathbb{E}_{z \sim q_\phi(z|x, h)} [\log(r_\phi(h_i|z))] \\ &\quad - \sum_i \sum_j w_{neg}^{(i,j)} D_{KL}(h_i, h_j) - \beta \sum_i D_{KL}(q_\phi(z|x, h_i) || p(z)) + const. \quad (8) \\ &= \sum_i w_{pos}^{(i)} \mathbb{E}_{z \sim q_\phi(z|x, h)} [\log(r_\phi(h_i|z))] - L_{ortho} - \beta L_{prior} + const.\end{aligned}$$

where β is a weight that controls the pressure on the distribution to match the prior approximation [18]. DELBO is a “looser” lower bound compared to the classic variational autoencoding ELBO [37], due to the extra orthogonality constraint that we add in a similar manner to how FactorVAE inserts the total correlation term in the ELBO [20], and the constant terms that are a product of our assumptions on the latent generative model and the connection of spaces h, z .

In practice, to avoid using a latent generative model we perform the latent reconstruction SSL task to maximize likelihood of individual h_i subspaces w.r.t h (or z) (see Supplementary Information ‘Self-supervised contrastive decomposition loss derivation and algorithm’) and optimize the below DELBO-inspired (L_{DELBOi}) objective:

$$\mathcal{L}_{DELBOi}(\phi; x, z, w_{pos}, w_{neg}, \beta) = L_{recon} + L_{ortho} - \beta L_{prior} \quad (9)$$

where the sign change of the L_{ortho} term in Eq.(9) is attributed to the cross-entropy trick that we employ to transform the $D_{KL}(h_i || h_j)$ term in Eq.(8) to a cross-entropy term CE_{neg} (Eq.(7)). Under this formulation (Eq.(9)), L_{recon} is a lower bound on the latent decomposition quality; the disentanglement of the latent space is maximized when the DELBO is maximized, which can happen if: 1) the approximate posteriors of the components latent spaces $q_\phi(h_i|x_i)$ collectively match the approximate posterior of the original signal’s latent space $q_\phi(h|x)$, 2) the L_{ortho} and $\sum D_{KL}$ terms vanish. By formulating this objective, we have essentially changed the variational inference problem to not rely on a reconstruction objective of the generative model, but in pursuing a latent reconstruction that is governed by prior distribution approximation and decomposition dynamics. The L_{recon} behaves indeed as a lower bound for the decomposition as is evident by our ablations in Supplementary Fig. 22. This is revealed by the divergence and cross entropy terms that represent the latent reconstruction and orthogonality terms L_{recon} and L_{ortho} that reach this lower bound plateau, after which disentanglement cannot be enhanced further. We can see how VDA parameters such as β , choice of decomposition method for D_w^C , input features type affect this DELBO (Supplementary Fig. 22). The collective optimization objective gives rise to variational decomposition autoencoding, graphically illustrated in Fig. 1c.

Multiple latent variables

DecVAE can simultaneously function as a single or multiple-branched model, depending on the number of time-scales expected in the problem at hand. Each branch acts as a recognition model ϕ , parameterized as a deep convolutional neural network that accepts as input sequences. Stochastic processes that construct complex non-stationary time series such as speech, often involve generative factors that can operate at the same or different time scales and thus a sequence can contain slow and fast varying attributes. DecVAE is invariant to the duration of the sequence and can accommodate multiple branches, where each branch handles a specific time-scale. Figure 1d demonstrates a dual branched DecVAE for speech, with the sequence branch operating in the timescale of seconds (utterances) and the frame branch operating in the timescale of milliseconds (phonetic content). As has been previously shown in speech-centric VAE designs (MFL-VAE [17], FHVAE [16]), speaker identity characteristics such as fundamental frequency or pitch $F0$, and volume have little to no variability across a sequence, whereas phonetic content has high variation within a sequence and is also affected by the speaker identity. To accommodate different time scales, we update the generative and inference models in the problem formulation by adding a second set of latent variables $\{t, t_1, t_2, \dots, t_C\}$ (Supplementary Information Fig. 3). Two different recognition models ϕ_z, ϕ_s are used to infer each timescale latent variable separately. It can be seen that ϕ_{h_s} operates in a plane of M sequences, whereas ϕ_{h_z} operates in a domain of $K^{(m)}$ frames for the current sequence m , making the latent variable S constant for the current m -th sequence.

It has been previously shown [17] that variational autoencoding can be extended to a second latent variable by assuming independency of generative factors in Z and S , and by applying a pooling operation across the input sequences T to end up with a single latent s_m for the m -th sequence. Accordingly, we modify DELBO in VDA and calculate the following quantity:

$$\begin{aligned} \mathcal{L}_{DualDELBO}(\phi_{h_z}, \phi_{h_s}; X, T, w_{pos}^{(i)}, w_{neg}^{(i)}, \beta_Z, \beta_S) = & \sum_i w_{pos}^{(i)} \mathbb{E}_{z \sim q_{\phi_{h_z}}(z|x, h_Z)} [\log(r_{\phi_{h_z}}(h_{iZ}|z))] \\ & + \sum_i w_{pos}^{(i)} \mathbb{E}_{s \sim q_{\phi_{h_s}}(s|x, h_S)} [\log(r_{\phi_{h_s}}(h_{iS}|s))] \\ & + L_{orthoH_Z} \\ & + L_{orthoH_S} \\ & - \beta_Z L_{priorZ} \\ & - \beta_S L_{priorS} \end{aligned} \quad (10)$$

where we use the same notation as the one used in Eq.(8) for the single-variable DELBO. In our experiments, we use the sequence-level variable S as support for variables that can be assumed to be invariant in the frame-level, such as speaker identity and emotion (Figures 2,5), as a natural disentanglement mechanism due to the design of the network. In terms of optimization, we see that the sequence branch behaves similarly to the frame branch in terms of training and convergence of the DELBO (Supplementary Fig. 22b,c). Prior approximation slows down convergence in the sequence branch as well, an effect that is apparent in the divergence and prior approximation loss terms (Supplementary Fig. 22b). Moreover, training a DecVAE with two branches has an influence on the Z -branch, as Z is influenced by S and this is evident through a slower convergence of Z in the case of a dual model, as Z has to also assimilate information from S in the joint training scenario (Supplementary Fig. 22c).

Decomposition model and self-supervised learning masking

As was analyzed in 'Self-supervised latent decomposition', the decomposition model \mathcal{D}_w^C is a key component in DecVAE; in our implementations we position \mathcal{D}_w^C as the first processing layer in the DecVAE architecture (Supplementary Fig. 2). \mathcal{D}_w^C is a signal processing module that can be incorporated into deep learning models, following a recent trend in the time-series representation learning literature [6, 14, 38]. \mathcal{D}_w^C receives a batched input of signals $X = \{X_1, X_2, \dots, X_B\}$, where B is the batch size and outputs a batch $X' = \{X_1^{C+1}, X_2^{C+1}, \dots, X_B^{C+1}\}$, where $X_b^{C+1} = \{X_b^{(0)}, X_b^{(1)}, X_b^{(2)}, \dots, X_b^{(C)}\}$ and $X_b^{(0)} \equiv X_b$. As hyperparameters w, C dictate the type of inductive bias that we use to achieve a satisfactory separation in the input domain X , we experiment with three different state-of-the-art decomposition algorithms: empirical wavelet transform (EWT) [22], empirical mode decomposition (EMD) [29], variational mode decomposition (VMD) [30]. Incorporation of these methods into deep learning models requires a fast and robust approach that can be applied at scale across large datasets. To that end, we also design a simple filter-based decomposition (FD) that is not based on some iterative optimization objective (Supplementary Alg. 3). FD uses infinite-impulse response (IIR) filters with fixed frequency-domain boundaries, applies a peak detection algorithm inside each fixed interval, and merges the detected peaks across individual intervals. As the number of detected peaks can be greater than the specified C , components are then merged based on a pre-defined strategy. For real data processing, we merge components from higher frequency intervals and keep lower frequency components intact. For simulations, we merge components across the whole spectrum with their nearest neighbors. The detailed decomposition module algorithm and the FD are presented in Supplementary Alg. 3. Standard hyperparameters for the decomposition model are tabulated in Supplementary Table 4.

FD is a fast approach to apply over big volumes of data as it only relies on simple filtering. Moreover, as the disentanglement properties of the latent space are affected by the input decomposition, FD ensures maximal orthogonality compared to the other methods, since filters are frequency-domain orthogonal by design, in contrast to time-frequency approaches like the EWT and time-domain approaches like the EMD. This property of FD prevents correlation of the components in the input domain that can propagate in the latent space and worsen the disentanglement quality (Supplementary Fig. 9). \mathcal{D}_w^C with FD is able to successfully recover properties of real and simulated formants, indicating good performance across simulated and real speech alike (Supplementary Fig. 4e,f,g,h). Hyperparameters and their values for all used decomposition methods are presented in Supplementary Table 4. Most importantly, FD is ideal for SSL as it is applying a "frequency-domain masking", as filters "mask" fixed frequency intervals. \mathcal{D}_w^C incorporates the concept of masking as an augmentation for the success of SSL training (Supplementary Alg. 2). Masking has been successfully applied as a pre-text task in SSL to create alternate views of an input that are then fed into a neural network, accompanied by an objective that encourages similarity of representations of different views of the same input [39] and has been found to be critical in learning informative representations. Here, the "mask" is applied in the frequency domain of the input, and the alternate views of the input constitute the components; this allows us to formulate "positive" and "negative" pairs, between the original signal and the components and enforce their similarity and dissimilarity in the latent space, and calculate the training objective losses based on that as was shown in 'Self-supervised latent decomposition'. As it has also been shown in the SSL literature [40, 41, 42], we validate that it is beneficial to "mask" and subsequently use about 50% of the available data at each step for the loss calculation (Supplementary Fig. 25).

Aggregation of latent subspaces

As was mentioned in the introductory part of Methods, the approximation \tilde{Z} of the true prior distribution Z requires an aggregation operation over the decomposed subspaces $\{\tilde{z}^0, \tilde{z}^1, \dots, \tilde{z}^C\}$. We experimented with different aggregation functions, i.e.: i) using individual subspaces and discarding the others, ii) concatenation of all components' subspaces, i.e., $z = [\tilde{z}^1, \tilde{z}^2, \dots, \tilde{z}^C]$, iii) concatenation of all components' and the original's subspaces $z = [\tilde{z}^0, \tilde{z}^1, \tilde{z}^2, \dots, \tilde{z}^C]$, and iv) a learned projection of the concatenated subspaces, i.e., $z = g([\tilde{z}^1, \tilde{z}^2, \dots, \tilde{z}^C])$, where $g(\cdot)$ is parameterized as a two-layered fully-connected network with non-linearity. Our results on our simulated data suggest that option (iii) yields an embedding of higher quality across all disentanglement and classification metrics, for different decomposition methods (FD,EWT) and values of prior approximation pressure $\beta = (0, 0.1, 1)$ (Supplementary Fig. 26).

Optimization and Pre-training

DecVAE models are trained on a single NVIDIA RTX 6000 Ada Generation hardware with a dual learning schedule and a batch size of about 1 minute of data. The sequence branch S trains with a linear schedule up to a peak learning rate of $1 * 10^{-4}$, whereas the frame branch Z trains with a constant schedule to a peak learning rate of $8 * 10^{-5}$; in both branches the learning rate is warmed up to its maximal value for 20 epochs and in the S branch the learning rate is decayed after that. The Adam optimizer is used [37] and training is monitored for early stopping by keeping track of improvement τ_δ with a patience of $\tau_{patience} = 5$ epochs on the total loss in the validation set requiring $\tau_\delta > 0.2\%$, after an initial period of $\tau_{warmup} = 100$ epochs. A maximum number of $t_{max} = 150$ epochs is set, but most models converge around 100-110 epochs (Supplementary Fig. 22,24).

Decomposition Variational Autoencoder

In the previous Methods sections we layed out the theoretical background and the functionality of important components in VDA and practical considerations for constructing a suitable optimization objective for learning disentangled representations. Here, we present how the collective functionality of individual components is organized into the DecVAE neural network architecture (Supplementary Fig. 2). DecVAE parameterizes the inference model q_ϕ as a parameter collection ϕ of a convolutional encoder and two projectors, with the decomposition model \mathcal{D}_w^C acting as a fixed recognition front-end; \mathcal{D}_w^C decomposes input frames from X into C components in X' and applies a random masking operation that marks a user-specified percentage of frames $l_{SSL\%}$ to be used in the DELBO calculation in Eq. (9). Mel filterbank features [16, 17] with a filterbank size $M = 80$ are then extracted for all components and the original signals in the batch B , as they were found to perform better on downstream tasks than raw waveforms (Supplementary Tables 6,7,8). A Wav2Vec2-based [40] shared encoder $f_W(\cdot)$ is then utilized for further feature extraction and projection of the signals through a seven-layered convolutional stack with Layer-Norm normalizations [43] and Gaussian Error Linear Units (GELU) [44] in an intermediate space $V^{v \times N}$. A shared hidden fully-connected projector $f_H(\cdot)$ with GELU non-linearity projects the encoder output in the space $H^{d \times N}$ where the L_{recon} and L_{ortho} are calculated by contrasting embeddings according to Eq. (6). Then, $C + 1$ latent projections $f_L(\cdot)^{(C+1)}$ with fully-connected linear layers $mu, logvar$ projects the embeddings to their latent subspaces \tilde{Z} where the prior approximation term in DELBO (Eq. (9)) is enforced for every subspace of dimension z_{dim} separately. Finally, the aggregator $g(\cdot)$ projects the subspaces to the final disentangled space $Z^{z_{dim} \times K \times N}$. It should be noted that all learnable parameters except the latent projectors $f_L(\cdot)^{(C+1)}$ are shared for all components and the

original signal, i.e., there is a single branch that handles all inputs. For a standard DecVAE single latent variable Z architecture, we choose values $v = 512$, $d = 512$, $z_{dim} = 48, 64$ for simulated and real speech, respectively, and $K = C + 1$ by using as an aggregation function the concatenation of all latent subspaces. In Algorithm 1 we describe the training process of DecVAE under the most successful experimental set of parameters (Supplementary Table 3).

Algorithm 1 DecVAE

Input: X

Params: $d_{max}, d_{min}, \mathcal{D}_w^C, C, \beta, l_{SSL\%}, z_{dim}, t_{max}, \tau_{warmup}, \tau_\delta, \tau_{patience}$

Output: Z

```

1: Discard sequences in  $X$  smaller than  $d_{min}$ 
2: Zero-pad sequences in  $X$  larger than  $d_{min}$  and smaller than  $d_{max}$ 
3: Concatenate randomly sequences in  $X$  larger than  $d_{max}$  to  $d_{max}$ 
4: Normalize sequences to mean of 0 and variance of 1
5:  $\tau_{current} \leftarrow 0, \tau_{count} \leftarrow 0$ 
6:  $l_{best} \leftarrow \infty$ 
7: Initialize  $f_W(\cdot), f_H(\cdot), f_L(\cdot)^{(C+1)}$  weights with He initialization
8: while  $t_{current} < t_{max}$  and  $\tau_{count} < \tau_{patience}$  do
9:    $x_b \leftarrow next(X), x_b \in R^{B,C+1,F,L}$ 
10:   $x'_b \leftarrow \mathcal{D}_w^C(x_b), mask \leftarrow sample(x_b, l_{SSL\%}), X' \in R^{B,C+1,F,d_{max}/F}$ 
11:   $x'_b \leftarrow Mel(x'_b), X' \in R^{N,C+1,F,M}$ 
12:   $v_b \leftarrow f_W(x'_b) \in R^{B,C+1,F,V}$ 
13:   $h_b \leftarrow f_H(v_b) \in R^{B,C+1,F,H}$ 
14:   $h_b^M \leftarrow h_b(mask)$ 
15:  Calculate  $L_{recon}, L_{ortho}$  on  $h_b^M$  via Eq. (7)
16:   $\tilde{z}_b \leftarrow f_L(h_b)^{(C+1)} \in R^{B,C+1,F,z_{dim}}$ 
17:   $z_b^M \leftarrow z_b(mask)$ 
18:  Calculate  $L_{prior}$  on  $z_b^M$  via Eq. (8)
19:   $\mathcal{L}_{total\_DELBO_i} \leftarrow L_{recon} + L_{ortho} - \beta * L_{prior}$ 
20:  if  $\tau_{current} \geq \tau_{warmup}$  then
21:    if  $\frac{|L_{total} - l_{best}|}{l_{best}} > \tau_\delta$  then
22:       $l_{best} \leftarrow L_{total}$ 
23:       $\tau_{count} \leftarrow 0$ 
24:    else
25:       $\tau_{count} \leftarrow \tau_{count} + 1$ 
26:    end if
27:  end if
28:  Update  $f_W(\cdot), f_H(\cdot), f_L(\cdot)^{(C+1)}$  using Adam on  $\mathcal{L}_{total\_DELBO}$ 
29:   $t_{current} \leftarrow t_{current} + 1$ 
30: end while
31:  $Z \leftarrow g(f_L(f_H(f_W(Mel(\mathcal{D}_w^C(X)))))))$ 

```

Disentanglement evaluation

To assess the disentanglement quality of the learned latent spaces we employ an array of different disentanglement metrics; disentanglement is an elusive and multi-faceted property and disentangled representation learning literature has given multiple definitions and ways of interpreting disentanglement [28, 45, 25], with different metrics

measuring different properties that a disentangled representation should have. Formulas for the utilized metrics are provided in Supplementary Information section ‘Disentanglement metrics’.

Mutual information

We calculate the mutual information (MI) metric [45] between all pairs of latent dimensions in Z . Although this metric is unsupervised and cannot be linked to the disentanglement performance across specific generative factors, it can give us information on how well the information is allocated across different dimensions in the latent spaces. The mutual information is calculated on the whole representation Z from the evaluation sets, based on discretization of the latent space through a histogram with 30 bins. MI is lower bounded by 0 and a representation with a MI close to 0 has dimensions with different information content.

Gaussian correlation

As a second unsupervised metric we calculate the normalized total correlation based on fitted Gaussian [28] or Gaussian correlation normalized (GCN). The covariance matrix and the mean vector of the latent space Z after encoding the whole evaluation set is calculated, and the KL divergence is calculated between a Gaussian with covariance matrix and mean vector equal to Z , and the product of this Gaussian’s marginals. We scale this quantity by the product of the dimension of Z with the average covariance for a fair comparison between models with different dimensionality in Z . GCN is lower bounded by 0 and a representation with a GCN close to 0 has less correlated dimensions.

Disentanglement, completeness, informativeness

Disentanglement, completeness and informativeness (DCI) is a framework that was proposed as a complete tool that assesses all properties of a disentangled representation through the three metrics [23]. Disentanglement measures the the property of modularity, that denotes independence between generative factors, when one of them varies. Completeness measures the property of compactness or completeness, that is maximized as fewer latent dimensions encapsulate information about single factors. Informativeness measures the property of information content or explicitness, that is exemplified when a generalizable relation is learned between factors (labels) and latent codes. DCI is a predictor-based framework, where predictors are trained to infer factors from the latent code to quantify informativeness, and the predictor’s inner parameters are used to infer the importance of each dimension in the latent code in predicting each factor. All three metrics evaluate in the $[0, 1]$ range.

Modularity and explicitness

Modularity and explicitness [24] is another framework proposed to measure the properties of modularity (disentanglement) and explicitness (informativeness). For modularity, the MI is calculated between factors and latent dimensions. For each dimension, the maximum MI is compared to all other MI scores with other generative factors. This is repeated for every dimension and the final modularity is the average over all dimensions. For explicitness, a Logistic Regression classifier is trained on the latent code per generative factor and the AUROC score is calculated. The final explicitness score is the average AUROC across all classes for all factors that is normalized to obtain a score from 0 to 1. Modularity and explicitness evaluate in the $[0, 1]$ range.

Interventional robustness score

Interventional robustness score (IRS) or robustness [25] has been proposed to isolate causal effects of a generative factor that are overlooked through other metrics due to confounding biases. Robustness is assessed by performing interventions (shuffling) on the generative factors associated with observations, while keeping observations of a specific factor fixed. High robustness is measured when changes in other factors do not affect the distance between the fixed-factors reference set and a second intervention set when other factors are changed. IRS evaluates in the $[0, 1]$ range.

Task-specific evaluation

We also evaluate our models in terms of their ability to learn meaningful representations for downstream classification tasks in the domains of speech recognition, emotion recognition and amyotrophic lateral sclerosis (ALS) dysarthria evaluation from speech. For the task-specific evaluation, we operate directly on the latent spaces Z and S by using simple linear (Logistic Regression) and non-linear (Random Forest, Support Vector Machine) classifiers to assign as little value as possible to the classifier and exemplify the quality of the learned representation.

Weighted and unweighted accuracy

We use weighted accuracy to measure task-specific performance in our experiments in the tasks of: vowel recognition, speaker identification, phoneme recognition, emotion recognition, disease duration prediction, clinical stage prediction. For emotion recognition, we also calculate unweighted accuracy as a standard metric in the IEMOCAP dataset [46] to account for emotion imbalance.

Weighted and macro-F1 score

We calculate weighted and macro-F1 score for the tasks mentioned in the previous accuracy paragraph. Real-world datasets have class distribution imbalances that cannot be captured by the accuracy metrics.

Cross-validation and confidence intervals

All classification tasks are performed in an outer five-fold cross-validation scheme with an inner three-fold cross-validation for classifier parameters selection, for five different classifier random initializations, except emotion recognition in IEMOCAP [34] that is performed in a leave-one-speaker-out outer cross-validation scheme with ten different random initializations. SimVowels is also excluded from confidence interval calculation as the data and class distribution is balanced and uniform by design. The metrics at each fold and random state are used to calculate 95% confidence intervals over all iterations of the classification. For the models' pre-training phase, we use a defined train and development set for all datasets; for SimVowels we use a $N = 4000$ utterances training set and $N = 500$ utterances development set. For pre-training on TIMIT [31] we use the standard TIMIT training and development sets. For fine-tuning on IEMOCAP we use a stratified speaker-emotion split and hold 90% of the data as a training set and 5% of the training set as a development set. In the evaluation phase we use the whole datasets.

For disentanglement metrics DCI, modularity and explicitness, that include training of predictors on the latent representations, we perform a five-fold cross-validation for five different random initializations that dictate the data split into training and test sets. We calculate 95% confidence intervals for these metrics across cross-validation

iterations and random initializations. Our results showed an enhanced robustness of the examined metrics in using different subsets of the TIMIT [31], VOC-ALS [3] and IEMOCAP [34] datasets for quantifying disentanglement in DecVAEs and supporting methods, manifesting with CIs below ± 0.001 (Supplementary Tables 9, 10, 12).

Hyperparameters

DecVAE involves selecting parameters both for the decomposition model \mathcal{D}_w^C and the neural network. Values for all parameters for training DecVAE and supporting methods used in both simulations and real data processing are presented in Supplementary Tables 3, 4, 5.

Datasets

We apply DecVAE and supporting VAE [10], β -VAE [18], ICA [26, 47], PCA [27, 47], kernel-PCA [48] methods to four audio datasets.

SimVowels

SimVowels is a simulated toy audio dataset inspired from [17] that models speakers as variations in a vocal tract factor and vowels as unique superpositions of three narrow-band formant carriers; it features $N = 4800$, 4 second sentences from 60 simulated speakers. Each speaker randomly utters one of five vowels ($/a/, /e/, /I/, /aw/, /u/$) with fast within-utterance one second alterations from vowel to vowel. SimVowels features two generative factors, the frame-level vowel uttered and the sequence-level speaker identity. The simulated vowels have the same structure and frequency-domain properties as real vowels [32] (Supplementary Fig. 4) and are thus a good fit to examine the ability of VAE models to disentangle factors of frequency-related generative processes. Details about SimVowels generation process are given in Supplementary Alg. 1.

TIMIT

TIMIT [31] is a corpus of broadband read American English speech with $N = 4056$ utterances with a maximum duration of 7.15 seconds, from 630 speakers. Development of phoneme recognition models uses 48 phoneme classes in TIMIT, but evaluation is made by appropriate mapping on a smaller set of 39 classes [49]. TIMIT has also two known generative factors of phoneme and speaker identity.

VOC-ALS

VOC-ALS [3] is an audio database of ALS patients and healthy controls for evaluating dysarthria severity. VOC-ALS has $N = 1224$ sentences with a maximum duration of 15 seconds where 153 participants perform a sustained repetition of the phonemes ($/a/, /e/, /i/, /o/, /u/, /pa/, /ta/, /ka/$). The clinical variables in VOC-ALS contain rich information about disease duration, progression and other details, as well as scores in various questionnaires. We use VOC-ALS to test DecVAE in generative processes involving three known factors, that are phoneme, speaker and disease staging. We utilize the disease duration and King’s clinical stage variables as disease staging indicators.

IEMOCAP

IEMOCAP [34] is an audio database of acted and improvised conversations where actors engage in conversations while exhibiting a range of emotional responses. IEMOCAP has $N = 5531$ utterances of 7 seconds maximum duration, from five two-person conversations and emotion annotations per utterance. We use IEMOCAP as another test for DecVAE in a three-factor generative process, where beside phoneme (48 phoneme classes) and speaker (10 speakers), the categorical emotion (angry,happy,neutral,sad) is the third generative factor.

Applications

Disentanglement quality evaluation

The ability of a model to learn disentangled representations that can separate underlying varying factors in complex, non-stationary and high-dimensional data such as time-series, is an important property that can amortize the data requirements and scale of neural networks in various tasks. Disentanglement of a representation can aid in interpretability and explainability of a neural network bringing a deeper understanding and knowledge of the mechanisms underlying time series phenomena and can also prove beneficial for improving classification performance in various predictive tasks. Given a dataset X we learn representations Z, S by applying DecVAE on the frame and sequence level as in ‘Decomposition Variational Autoencoder’ and Alg.1. We evaluate the quality of representations in several aspects by using the eight different metrics as described in ‘Disentanglement evaluation’ and the annotations provided in the datasets. We also examine the visual quality of the learned spaces by learning and visualizing low-dimensional manifolds of the high-dimensional Z, S spaces through TSNE [21]. For SimVowels and TIMIT, we evaluate disentanglement on the combined development and test sets, with the training set being used only in the pre-training phase.

Speech recognition

We perform the phoneme and speaker identification tasks in the SimVowels dataset as a more practical complement to the more theoretical disentanglement quality evaluation. As a toy dataset with generative factors that are fully expressed through frequency-domain properties, SimVowels serves as a controlled experiment that validates the need for variational decomposition autoencoding and demonstrates a case where conventional VAE models fail. Generalization of the performance in both vowel and speaker recognition with the additional constraint of interpretability is the goal of this experiment, and where we show that VAE models struggle. We demonstrate in Results the increased efficiency of DecVAE models in achieving increased qualitative and quantitative speech disentanglement performance in Figures 2,3 and Supplementary Tables 6, 7, 8, 9. We also perform speech recognition in VOC-ALS and IEMOCAP where a third factor that is not related to speech dynamics is involved, and show how DecVAE has increased capacity in generalizing disentanglement to more factors without losing speech recognition capacity (Fig. 4,5, Supplementary Tables 11,10,12, 13). For the SimVowels dataset we evaluate speech recognition on the combined development and test sets, with the training set being used only in the pre-training phase.

Transfer learning

We also examine the scenario where DecVAE and VAE models are pre-trained on a dataset X , then the pre-trained DecVAE is used to embed a dataset Y in latent spaces Z, S . We test both the zero-shot transfer learning scenario

when no adaptation of the DecVAE parameters to the new dataset Y is performed, as well as the fine-tuning scenario where a fine-tuning phase using the VDA framework is performed on Y according to Alg.1 to adjust the DecVAE parameters, before proceeding to the evaluation phase. For the transfer learning experiments we use the DecVAE models trained on SimVowels and TIMIT.

Zero-shot dysarthria severity evaluation

We evaluate dysarthria severity as a classification task to predict disease duration and King’s clinical stage [33] and as a disentanglement task involving three generative factors of phoneme, speaker and the King’s stage that describes disease progression according to failure of anatomical body systems. We utilize the zero-shot transfer learning scheme by transferring models from SimVowels and TIMIT. Dysarthria arises as an effect of vocal tract degeneration and thus is a phenomenon that can be described by alterations in the structural and frequency-domain properties of the speech production system. We explore the capacity of DecVAE and VAE models in capturing the different factors involved in dysarthria in Results through disentanglement and task-specific evaluations (Fig. 4, Supplementary Tables 11,10). We do not split VOC-ALS in sets but rather perform the cross-validation evaluation on the whole dataset.

Speech emotion recognition fine-tuning evaluation

We evaluate emotion recognition performance in relation to speaker and phoneme identification by transferring models and fine-tuning them on IEMOCAP before evaluation. We optimize \mathcal{L}_{DELB0} over a period of 25 epochs with a constant learning rate of $5 * 10^{-6}$ for both Z, S branches without early stopping. Emotion is an attribute not directly encoded in the frequency dynamics of the speech production system and thus presents a more challenging task than dysarthria severity in terms of disentanglement. In Results, we show how DecVAE learns emotionally resonant representations compared to other models (Fig. 5, Supplementary Tables 12, 13).

Latent response analysis and interpretability

For interpretability of the latent space dynamics and model response on different tasks, we perform a latent traversal and response analysis [18]. We collect small subsets from all four datasets where single generative factors are fixed and other factors are left variable. We then apply DecVAE on these subsets without training and collect the set of dimensions $Z_t \in Z, Z_t \subset Z$ that demonstrate the larger and lower variance. We then draw the latent amplitude of the DecVAE responses to each pair of factors to demonstrate how traversing single factor dimensions is reflected on single latent dimensions z_t . This analysis provides insight on how VDA differs from variational autoencoding, and how DecVAE allocates information for different combinations of generative factor values in different dimensions, in a way that promotes disentanglement and informativeness (Fig. 6a,b,c, Supplementary Fig. 18,19,20,21).

Data Availability

The pseudo-code for generating SimVowels is provided in Supplementary Alg.1 and Python code is also available in our publicly available codebase at <https://github.com/GiannisZgs/DecVAE>. We also make the SimVowels dataset publicly available for downloading at <https://drive.google.com/drive/folders/1Fl8Euwfv-rENiNDAQWm3gd0L3IifqFD?usp=sharing>. TIMIT can be downloaded from <https://catalog.ldc.upenn.edu/LDC93S1>.

VOC-ALS can be downloaded from <https://www.synapse.org/Synapse:syn53009474/wiki/624730>. IEMOCAP can be downloaded from <https://sail.usc.edu/iemocap/>.

Code Availability

We release a codebase in a detailed format with usage scenarios to reproduce results of this work, but also to allow researchers and practitioners to apply, build upon and extend variational decomposition autoencoding. The codebase is available at <https://github.com/GiannisZgs/DecVAE> [50]. All code was implemented in R v.4.5.1 and Python v3.9.11 using PyTorch [51] and HuggingFace [52]. For disentanglement metrics implementation we used *disentanglement_lib* from Google Research [28]. The *ggbreak* [53] package was used for R visualizations.

Supplementary Information

The supplementary information file can be downloaded at <https://drive.google.com/drive/folders/1sZl2AcCtRK-1oav7XZSaxlu0Cq0-3MMs?usp=sharing>.

References

- [1] Fiser J., Berkes P., Orbán G., and Lengyel M. Statistically optimal perception and learning: from behavior to neural representations. *Trends in Cognitive Sciences*, **14**:119–130, (2010).
- [2] van den Oord A., Li Y., and Vinyals O. Representation Learning with Contrastive Predictive Coding. *Preprint at https://arxiv.org/abs/1807.03748*, (2018).
- [3] Dubbioso R. et al. Voice signals database of ALS patients with different dysarthria severity and healthy controls. *Scientific Data*, **11**:1–14, (2024).
- [4] Chen X., Xu X., Kamihigashi T., Chen J., Zhang Z., Takiguchi T., and Hancock E.R. Speaker-Independent Emotional Voice Conversion via Disentangled Representations. *IEEE Transactions on Multimedia*, (2022).
- [5] Isomura T. and Toyoizumi T. Dimensionality reduction to maximize prediction generalization capability. *Nature Machine Intelligence*, **3**:434–446, (2021).
- [6] Woo G., Liu C., Sahoo D., Kumar A., and Hoi S. CoST: Contrastive Learning of Disentangled Seasonal-Trend Representations for Time Series Forecasting. *International Conference on Learning Representations*, (ICLR, 2022).
- [7] Kay K., Jamison K.W., Zhang R.Y., and Uğurbil K. A temporal decomposition method for identifying venous effects in task-based fMRI. *Nature Methods*, **17**:1033–1039, (2020).
- [8] Cohen N.K., Huang X., and Wang D. Joint variational autoencoders for multimodal imputation and embedding. *Nature Machine Intelligence*, **5**:631–642, (2023).
- [9] Ridgeway K. A Survey of Inductive Biases for Factorial Representation-Learning. *Preprint at https://arxiv.org/pdf/1612.05299*, (2016).

- [10] Kingma D. P. and Welling M. Auto-Encoding Variational Bayes. In *International Conference on Learning Representations*, (ICLR,2014).
- [11] Rolinek M., Zietlow D., and Martius G. Variational Autoencoders Pursue PCA Directions (by Accident). *Proceedings of the IEEE Computer Society Conference on Computer Vision and Pattern Recognition*, pages 12398–12407, (2018).
- [12] Apostolidis G.K. and Hadjileontiadis L.J. Swarm decomposition: A novel signal analysis using swarm intelligence. *Signal Processing*, **132**:40–50, (2017).
- [13] Hyvarinen A. and Morioka H. Unsupervised Feature Extraction by Time-Contrastive Learning and Nonlinear ICA. *Advances in Neural Information Processing Systems*, **29**, (2016).
- [14] Boris N. Oreshkin, Dmitri Carpov, Nicolas Chapados, and Yoshua Bengio. N-BEATS: Neural basis expansion analysis for interpretable time series forecasting. *International Conference on Learning Representations*, (ICLR, 2020).
- [15] Mathieu E., Rainforth T., Siddharth N., and Teh Y.W. Disentangling Disentanglement in Variational Autoencoders. *International Conference on Machine Learning*, pages 7744–7754, (PMLR, 2019).
- [16] Hsu W.N., Zhang Y., and Glass J. Unsupervised Learning of Disentangled and Interpretable Representations from Sequential Data. *Advances in Neural Information Processing Systems*, pages 1879–1890, (2017).
- [17] Boulian G. A Study of Inductive Biases for Unsupervised Speech Representation Learning. *IEEE/ACM Transactions on Audio Speech and Language Processing*, **28**:2781–2795, (2020).
- [18] Higgins I. et al. beta-VAE: Learning Basic Visual Concepts with a Constrained Variational Framework. In *International conference on learning representations*, (ICLR, 2017).
- [19] Chen R.T.Q., Li X., Grosse R.B., and Duvenaud D.K. Isolating Sources of Disentanglement in Variational Autoencoders. *Advances in Neural Information Processing Systems*, **31**, (2018).
- [20] Kim H. and Mnih A. Disentangling by factorising. *International Conference on Machine Learning*, **80**:2649–2658, (PMLR, 2018).
- [21] van der Maaten L. and Hinton G. Visualizing data using t-sne. *Journal of machine learning research*, **9**:2579–2605, (2008).
- [22] Gilles J. Empirical wavelet transform. *IEEE Transactions on Signal Processing*, **61**(16):3999–4010, (2013).
- [23] Eastwood C. and Williams C.K.I. A Framework for the Quantitative Evaluation of Disentangled Representations. In *International Conference on Learning Representations*, (ICLR, 2018).
- [24] Ridgeway K. and Mozer M.C. Learning Deep Disentangled Embeddings With the F-Statistic Loss. *Advances in Neural Information Processing Systems*, **31**, (2018).
- [25] Suter R., Miladinovic D., Schölkopf B., and Bauer S. Robustly Disentangled Causal Mechanisms: Validating Deep Representations for Interventional Robustness. *Proceedings of the 36th International Conference on Machine Learning*, **97**:6056–6065, (PMLR,2019).

[26] A. Hyvärinen, Hurri J., and Hoyer P.O. Independent component analysis. In *Natural Image Statistics: A Probabilistic Approach to Early Computational Vision*, pages 151–175. Springer, (2001).

[27] Greenacre M., Groenen P.J.F., Hastie T., D’Enza A.I., Markos A., and Tuzhilina E. Principal component analysis. *Nature Reviews Methods Primers*, **2**:1–21, (2022).

[28] Locatello F., Bauer S., Lucic M., Raetsch G., Gelly S., Schölkopf B., and Bachem O. Challenging Common Assumptions in the Unsupervised Learning of Disentangled Representations. *Proceedings of the 36th International Conference on Machine Learning*, **97**:4114–4124, (PMLR,2019).

[29] Huang N.E. et al. The empirical mode decomposition and the hilbert spectrum for nonlinear and non-stationary time series analysis. *Proceedings of the Royal Society of London. Series A: mathematical, physical and engineering sciences*, **454**(1971):903–995, (1998).

[30] Dragomiretskiy K. and Zosso D. Variational mode decomposition. *IEEE Transactions on Signal Processing*, **62**(3):531–544, (2014).

[31] Garofolo J.S. et al. Timit acoustic-phonetic continuous speech corpus. *LDC93S1 Philadelphia: Linguistic Data Consortium*, (1993).

[32] Ladefoged P., Johnson K., and Ladefoged P. *A course in phonetics*, volume 3. Thomson Wadsworth Boston, 2006.

[33] Roche J.C. et al. A proposed staging system for amyotrophic lateral sclerosis. *Brain*, **135**:847–852, (2012).

[34] Busso C. et al. IEMOCAP: Interactive emotional dyadic motion capture database. *Language Resources and Evaluation*, **42**:335–359, (2008).

[35] Menéndez M.L., Pardo J.A., Pardo L., and Pardo M.C. The Jensen-Shannon divergence. *Journal of the Franklin Institute*, **334**(2):307–318, (1997).

[36] Jing L., Vincent P., LeCun Y., and Tian Y. Understanding Dimensional Collapse in Contrastive Self-supervised Learning. *International Conference on Learning Representations*, (ICLR,2022).

[37] Kingma D.P. and Ba J.L. Adam: A Method for Stochastic Optimization. *International Conference on Learning Representations*, (ICLR, 2015).

[38] Zhou T., Ma Z., Wen Q., Wang X., Sun L., and Jin R. FEDformer: Frequency Enhanced Decomposed Transformer for Long-term Series Forecasting. pages 27268–27286. PMLR, (2022).

[39] Balestrieri R. et al. A Cookbook of Self-Supervised Learning. *Preprint at <https://arxiv.org/abs/2304.12210v1>*, (2023).

[40] Baevski A., Zhou Y., Mohamed A., and Auli M. wav2vec 2.0: A Framework for Self-Supervised Learning of Speech Representations. *Advances in Neural Information Processing Systems*, **33**:12449–12460, (2020).

[41] Mohamied Y. and Bell P. Bootstrap Predictive Coding: Investigating a Non-Contrastive Self-Supervised Learning Approach. *IEEE International Conference on Acoustics, Speech and Signal Processing (ICASSP)*, pages 11541–11545, (2024).

[42] Grill J.-B. et al. Bootstrap your own latent-a new approach to self-supervised learning. *Advances in neural information processing systems*, **33**:21271–21284, (2020).

[43] Ba J.L., Kiros J.R., and Hinton G.E. Layer Normalization. *Preprint at <https://arxiv.org/pdf/1607.06450.pdf>*, (2016).

[44] Hendrycks D. and Gimpel K. Gaussian Error Linear Units (GELUs). *Preprint at <https://arxiv.org/pdf/1606.08415.pdf>*, (2016).

[45] Carbonneau M.A., Zaidi J., Boilard J., and Gagnon G. Measuring Disentanglement: A Review of Metrics. *IEEE Transactions on Neural Networks and Learning Systems*, **35**:8747–8761, (2022).

[46] Antoniou N., Katsamanis A., Giannakopoulos T., and Narayanan S. Designing and Evaluating Speech Emotion Recognition Systems: A Reality Check Case Study with IEMOCAP. *IEEE International Conference on Acoustics, Speech and Signal Processing (ICASSP)*, pages 1–5, (2023).

[47] Pedregosa F. et al. Scikit-learn: Machine learning in python. *The Journal of Machine Learning Research*, **12**:2825–2830, (2011).

[48] Schölkopf B., Smola A., and Müller K.R. Kernel principal component analysis. *Lecture Notes in Computer Science (including subseries Lecture Notes in Artificial Intelligence and Lecture Notes in Bioinformatics)*, **1327**:583–588, (1997).

[49] Lee K.F. and Hon H.W. Speaker-Independent Phone Recognition Using Hidden Markov Models. *IEEE Transactions on Acoustics, Speech, and Signal Processing*, **37**:1641–1648, (1989).

[50] Ziogas I.N., Al Shehhi A., Khandoker A.H., and Hadjileontiadis L.J. Variational decomposition autoencoding improves disentanglement of latent representations. *Zenodo, <https://doi.org/10.5281/zenodo.17773435>*, (2025).

[51] Paszke A. et al. Pytorch: An imperative style, high-performance deep learning library. *Advances in neural information processing systems*, **32**, (2019).

[52] Wolf T. et al. Transformers: State-of-the-art natural language processing. In *Proceedings of the 2020 Conference on Empirical Methods in Natural Language Processing: System Demonstrations*, pages 38–45, (EMNLP,2020).

[53] Shuangbin X., Chen M., Feng T., Zhan L., Zhou L., and Yu G. Use ggbreak to effectively utilize plotting space to deal with large datasets and outliers. *Frontiers in Genetics*, **12**, (2021).